RADC-TR-89-10
Final Technical Report
March 1989

A STUDY OF LOADED MICROSTRIP ANTENNAS AND THEIR APPLICATIONS TO ARRAYS

University of Houston

William F. Richards, Ajaz A. Khan, Stuart A. Long

ROME AIR DEVELOPMENT CENTER
Air Force Systems Command
Griffiss Air Force Base, NY 13441-5700

This report has been reviewed by the RADC Public Affairs Division (PA) and is releasable to the National Technical Information Service (NTIS). At NTIS it will be releasable to the general public, including foreign nations.

RADC-TR-89-10 has been reviewed and is approved for publication.

APPROVED: John R Corneil

JOHN R. CORNEIL, CAPT, USAF
Project Engineer

APPROVED: John K Schindler

JOHN K. SCHINDLER
Director of Electromagnetics

FOR THE COMMANDER: John A. Ritz

JOHN A. RITZ
Directorate of Plans & Programs

If your address has changed or if you wish to be removed from the RADC mailing list, or if the addressee is no longer employed by your organization, please notify RADC (EEAS) Hanscom AFB MA 01731-5000. This will assist us in maintaining a current mailing list.

Do not return copies of this report unless contractual obligations or notices on a specific document require that it be returned.

UNCLASSIFIED

SECURITY CLASSIFICATION OF THIS PAGE

REPORT DOCUMENTATION PAGE

Form Approved OMB No. 0704-0188

1a. REPORT SECURITY CLASSIFICATION UNCLASSIFIED	1b. RESTRICTIVE MARKINGS N/A
2a. SECURITY CLASSIFICATION AUTHORITY N/A	3. DISTRIBUTION/AVAILABILITY OF REPORT Approved for public release; distribution unlimited.
2b. DECLASSIFICATION/DOWNGRADING SCHEDULE N/A	
4. PERFORMING ORGANIZATION REPORT NUMBER(S) TR 87-13	5. MONITORING ORGANIZATION REPORT NUMBER(S) RADC-TR-89-10
6a. NAME OF PERFORMING ORGANIZATION University of Houston 6b. OFFICE SYMBOL (If applicable)	7a. NAME OF MONITORING ORGANIZATION Rome Air Development Center (EEAS)
6c. ADDRESS (City, State, and ZIP Code) Applied Electromagnetics Laboratory Department of Electrical Engineering Houston TX 77004	7b. ADDRESS (City, State, and ZIP Code) Hanscom AFB MA 01731-5000
8a. NAME OF FUNDING/SPONSORING ORGANIZATION Rome Air Development Center 8b. OFFICE SYMBOL (If applicable) EEAS	9. PROCUREMENT INSTRUMENT IDENTIFICATION NUMBER F30602-81-C-0202
8c. ADDRESS (City, State, and ZIP Code) Hanscom AFB MA 01731-5000	10. SOURCE OF FUNDING NUMBERS PROGRAM ELEMENT NO: 61102F; PROJECT NO: 2305; TASK NO: J3; WORK UNIT ACCESSION NO: P6
11. TITLE (Include Security Classification) A STUDY OF LOADED MICROSTRIP ANTENNAS AND THEIR APPLICATIONS TO ARRAYS	
12. PERSONAL AUTHOR(S) William F. Richards, Ajaz A. Khan, Stuart A. Long	
13a. TYPE OF REPORT Final 13b. TIME COVERED FROM Jun 86 TO Dec 86 14. DATE OF REPORT (Year, Month, Day) March 1989 15. PAGE COUNT 96	
16. SUPPLEMENTARY NOTATION N/A	

17. COSATI CODES			18. SUBJECT TERMS (Continue on reverse if necessary and identify by block number)
FIELD	GROUP	SUB-GROUP	Dynamic Impedance Tuning Microstrip Elements Phased Arrays
17	09		
20	14		

19. ABSTRACT (Continue on reverse if necessary and identify by block number)

An experimental study of reactively loaded rectangular microstrip antennas is presented in this report. The reactive loads used here were either a single pin, or a symmetrically located pair of pins, short circuiting points on the patch to corresponding points on the ground plane. A set of points forming a single curve for the case of one shorting pin or two symmetrically located curves for the case of two shorting pins was found. A single, or a pair of short circuits placed at any point on these curves results in an element having a fixed resonant frequency and a fixed radiation pattern independent of the point selected. The input impedance, however, varies over a very large range when a short circuit or pair of short circuits is moved along these curves. The major application of this work is the study of the feasibility of maintaining an impedance match for the elements of a microstrip antenna array with changing scan angle by moving the position of one or two short-circuiting pins. An experimental and theoretical study of the mutual impedance for microstrip array elements was conducted and used in a computer program simulating a finite array. (over)

20. DISTRIBUTION/AVAILABILITY OF ABSTRACT ☐ UNCLASSIFIED/UNLIMITED ☒ SAME AS RPT ☐ DTIC USERS	21. ABSTRACT SECURITY CLASSIFICATION UNCLASSIFIED
22a. NAME OF RESPONSIBLE INDIVIDUAL John R. Corneil, CAPT, USAF	22b. TELEPHONE (Include Area Code) (617) 377-2059 22c. OFFICE SYMBOL RADC (EEAS)

DD Form 1473, JUN 86 Previous editions are obsolete

SECURITY CLASSIFICATION OF THIS PAGE
UNCLASSIFIED

Block 19. Abstract (Cont'd)

Though the model used for mutual impedance was somewhat crude, the simulation program predicted a variation of active element impedance with scan angle. For a number of different scan angles, the position of shorting pins was adjusted to obtain a match for all of the array elements thus indicating that this dynamic matching technique may be feasible for scanned arrays.

Contents

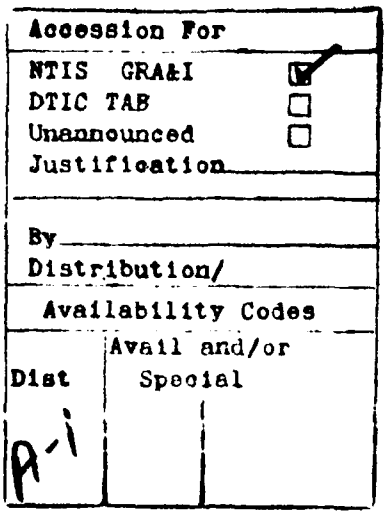

List of Figures

Chapter 1

INTRODUCTION

In recent years extensive research and development in microstrip antennas has led to a more thorough understanding of the application potential of microstrip radiators. This has also established the microstrip antenna as a special topic by itself in the field of microwave radiators. The idea of using a printed conductor on a substrate as a radiating element came from the microstrip transmission lines that were developed much earlier. The trend to miniaturize and integrate electronic systems has created a positive demand for this new generation of antennas. Over the years the many advantages offered by microstrip antennas have been used with good results. The main advantages are light weight, low cost, planar configuration and compatability with integrated circuits [1]. Microstrip antennas can be loaded reactively to change the electric field distribution between the patch and the ground plane. By an appropriate choice of the type and location of the reactive loads a number of antenna parameters can be altered. For example, the resonant frequency can be shifted, dual bands of variable band separation can be made [2], the polarization can be altered [3] and modes producing completely different radiation patterns can be made to

resonate at the same frequency [4]. The reactive loads can be as complicated as resonant structures such as open-circuited or short circuited transmission lines or varactor diodes, or as simple as a short circuit (perhaps implemented as a PIN diode). The purpose of this work was to study the feasibility of using movable short-circuit loads to keep the elements matched in a scanned microstrip antenna array.

In the first part of this report such reactively loaded antennas are studied both theoretically and experimentally. Measurements were made on microstrip radiators with reactive loads positioned at various points on the patch. These experiments were done to verify the theory developed for such loaded elements at the Applied Electromagnetics Laboratory, Department of Electrical Engineering at the University of Houston [5]. The reactive loading was provided by short circuit loads (PIN diodes can also be used) and the radiation pattern and input resistance and reactance were measured.

The second part of the report is the simulation of a finite microstrip antenna array and the computation of the mutual coupling. This has been done for many different edge to edge separations of a pair of rectangular microstrip radiators; and the variation of the mutual impedance with distance for both the E-plane and the H-plane was computed and measured. Also, the variation of the mutual impedance in a linear array with more than two elements has been studied; and both computed and measured results have been obtained.

The effect on the active input impedance of electronic scanning by changing

the progressive phase shift angle between the array elements has also been computed. This change in element impedance is due to the mutual coupling between the elements of the array. The change in active impedance of microstrip elements in a scanned array causes power to be reflected back into the feed. The use of microstrip antenna elements with movable short circuit loads in order to match the microstrip antenna elements in a scanned array is studied. This could improve the array performance. A preliminary study of the feasibility of doing this is the main focus of this work. Before discussing the details of this study, a brief overview of microstrip elements is given in Section 1.1 and 1.2.

1.1 The microstrip antenna

A microstrip antenna is illustrated in Figure 1.1 in its simplest form. It has a radiating patch which is usually made of copper and a ground plane separated from the radiator by a dielectric substrate. The dielectric constant ϵ_r most popularly used is usually in the range of 2.0 to 10.0 . The actual choice of this depends on the specific application. For example, low frequency applications require high dielectric constants to keep the size small. Substrate choice and evaluation are an essential part of the design procedure of the microstrip antenna. The specific substrate properties of importance are the dielectric constant, the loss tangent, and the variation of both with temperature. Other factors include homogeneity, isotropicity, and dimensional stability [1]. The radiation from a microstrip antenna can, as an approximation, be attributed to the fringing field between the edge of the antenna and the ground plane. This is illustrated in Figure 1.2. Additional

information can be found in reference [1].

Microstrip antennas have many advantages and disadvantages compared with other standard antennas operating in their frequency range. Elements can be built having a center frequency which can range from 100 MHz to above 50 GHz [1]. They are typically low in cost and light in weight. They can be used to generate both linear and circular polarization. Dual frequency microstrip antennas can be easily made so that they can be used at different transmit and receive frequencies [6]. Also, the feed lines required for the antenna can be easily fabricated together with the antenna using the well-developed etching techniques used for making printed circuit boards.

On the other hand microstrip antennas have a narrow bandwidth. Also, the end fire performance (parallel to the plane of the patch) is very poor and they have a low power handling capacity [1]. There are also possibilities of the excitation of surface modes which lead to the loss of radiated power.

Microstrip antennas have a wide area of application. They can be used in Doppler radar systems, satellite communication, missile telemetry, feed elements in complex antennas and biomedical applications. The areas of applications are continuing to grow as the awareness of their use increases.

Microstrip antennas are modelled in many different ways with each model having its own advantages and disadvantages. The most popular models are the transmission line model [1], the cavity model (Lo *et al.*) [4], the wire grid model (Agarwal and Bailey) [1], and the modal expansion model (Carver and Coffey) [1]. There are several other models which have been developed, information on which can be found

in [1].

1.2 Design procedure

A general overview of the design of rectangular microstrip antennas is given and the relevant design expressions are stated. The first step in the design is to choose an appropriate dielectric constant. As mentioned before the frequency of operation has an important role to play in this selection. Some of the substrates that have been largely used are [1] rexolite ($\epsilon_r = 2.6$), duroid ($\epsilon_r = 2.32$) and alumina ($\epsilon_r = 9.8$). For a dielectric substrate with a thickness of h, it has been shown by Schroeder [6] that the practical width for an efficient radiator is

$$W = \frac{c}{2f_r}\left(\frac{\epsilon_r + 1}{2}\right) \tag{1.1}$$

The expression for the element length is

$$L = \frac{c}{2f_r\sqrt{\epsilon_r}} - 2\Delta l \tag{1.2}$$

where f_r is the desired resonant frequency, ϵ_r is the relative permittivity, c is the speed of light and Δl is given by

$$\Delta l = 0.412h\frac{(\epsilon_e + 0.3)(W/h + 0.264)}{(\epsilon_e - 0.258)(W/h + 0.8)} \tag{1.3}$$

where ϵ_e is the effective dielectric constant given by

$$\epsilon_e = \frac{(\epsilon_r + 1)}{2} + \frac{(\epsilon_r - 1)}{2}\left(1 + \frac{12h}{W}\right)^{-1/2} \tag{1.4}$$

in which W is the width of the antenna (see Figure 1.1).

Several authors have suggested different expressions for the radiation pattern of the rectangular microstrip radiator [1]. Richards *et al.* [7] have found good agreement between theoretically predicted values of input impedance and experimentally

obtained values using the cavity model approach. Expressions for other factors such as radiation resistance, quality factor, bandwidth, can be found in reference [1].

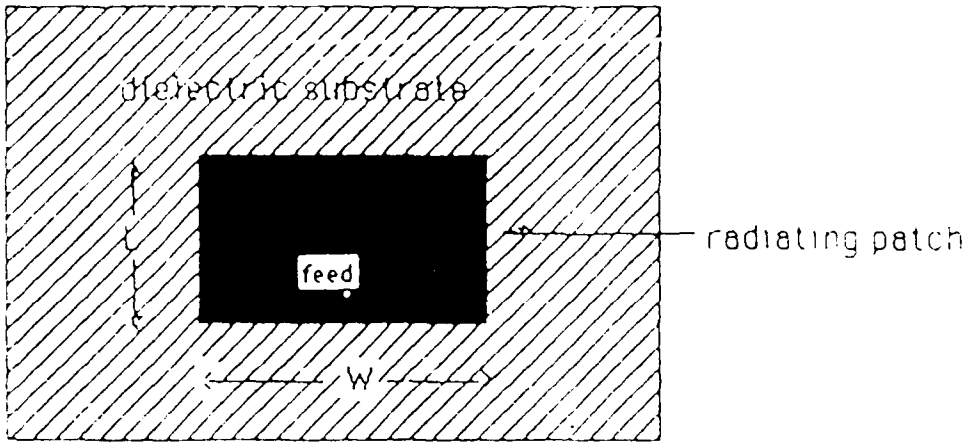

(a)

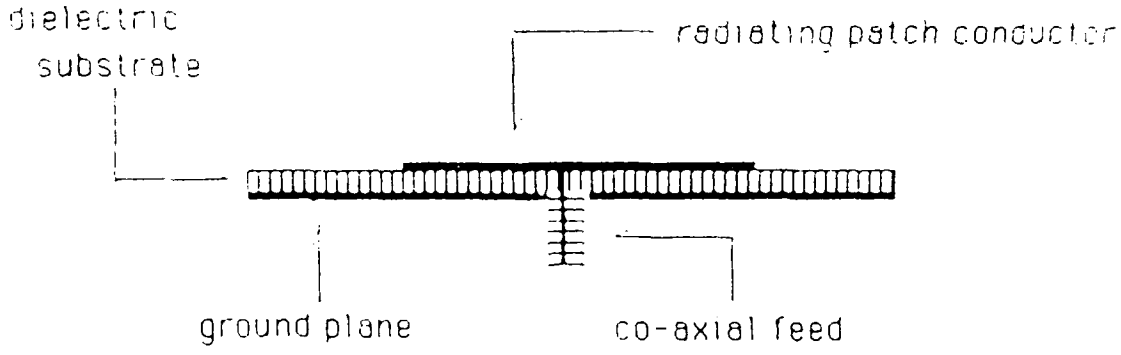

(b)

Figure 1.1: The microstrip antenna (a) top view (b) side view

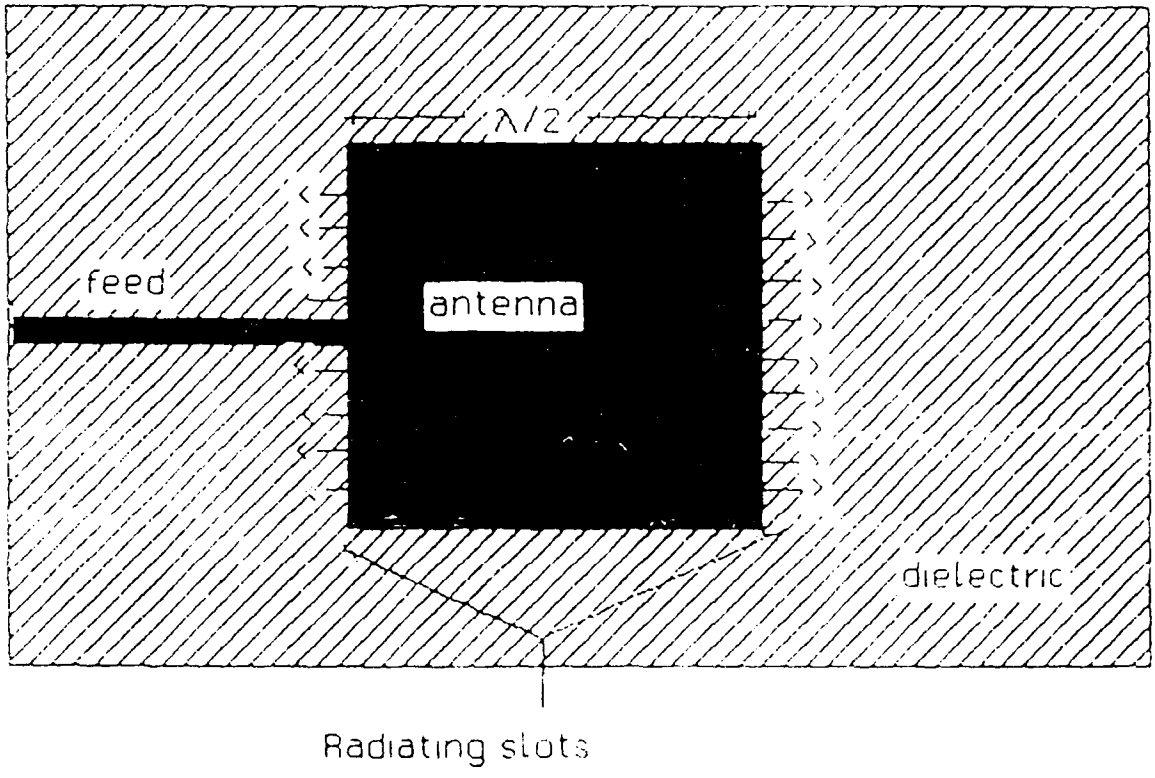

Figure 1.2: Radiation from the microstrip antenna showing the fringing fields

Chapter 2

LOADED MICROSTRIP ANTENNAS

By loading the microstrip antenna with shorting pins from the radiating surface to the ground plane the input impedance and resonant frequency can be changed over a wide range without affecting its radiation pattern. It is possible to change just the input impedance and keep the resonant frequency constant by placing the shorts along a properly chosen locus of points on the antenna patch. Both single and dual loads can be used to vary the input impedance, but as is shown in the experimental results, using dual loads yields a wider range of input impedance variation. Also, dual loads produce lower cross-polarization levels than single loads. The main purpose of this work was the study of using movable loads in a microstrip antenna array to control the input impedance variation of the individual elements as phase scanning takes place. The theory of these loaded microstrip elements is given here and is followed by experimental results.

2.1 Theory of loaded microstrip antennas

A brief overview is given in this section of the expressions developed by Richards [5] which are based on the cavity model analysis. The results that were obtained theoretically were verified by the author experimentally with excellent agreement.

In a microstrip antenna the existence of a source-free field at resonance implies the existence of a non-zero feed current. Kirchoff's voltage law applied to the lumped circuit model of Figure 2.1, which is a source-free microstrip cavity loaded at a single point with load reactance X_L implies

$$j(X_L + X_{in})I_L = 0, \tag{2.1}$$

where I_L is the load current and X_{in} is the input reactance of the loaded cavity. Richards [5] showed that X_{in} may be represented as

$$X_{in} = X_F + X_L \tag{2.2}$$

where X_F is feed reactance, X_{in} is the input reactance at the load point of an unloaded microstrip cavity.

All these reactances are functions of frequency and the roots are the resonant frequencies of the loaded element. The resonant mode usually used in microstrip antennas is the (0,1) mode. The normalized voltage distribution at the observation point (x, y) on the antenna for this mode is given by

$$V(x, y) = \cos\left(\frac{\pi y}{b}\right) \tag{2.3}$$

where the element dimensions are $a \times b$. This is zero on the center line $y = b/2$ of the patch. This line of zero field is called the node line. The addition of loads

on the microstrip antenna moves this nodal line closer to or further away from the feed point. The closer the nodal line is to the feed point the lower is the input impedance of the antenna and vice versa.

Multiple loads require the roots of

$$\det \begin{pmatrix} (Z_{11} + Z_L^{(1)}) + Z_{12} \dots Z_{1N} \\ Z_{12} \ (Z_{22} + Z_L^2) \dots Z_{2N} \\ \vdots \ \vdots \ \vdots \\ Z_{1N} \ Z_{2N} \dots (Z_{nn} + Z_L^{(n)}) \end{pmatrix} = 0 \tag{2.4}$$

where Z_{ij} is the z-parameter between the i^{th} and the j^{th} port of a multiple port microstrip cavity, and Z_L^i is the load impedance connected to the i^{th} port. One can solve these characteristic equations numerically for the resonant frequency. The input impedance, voltage distribution and the radiation pattern can then be found as described in [7]. Additional information can be found in reference [5].

2.2 Computed and measured results

For short circuit reactive loads we have $X_L = 0$. Extensive experiments were performed to study the effect of short circuit loading on the characteristics of a microstrip antenna. All experiments were done using 3M Corporation's CuClad 250 glass reinforced double clad PTFE with a dielectric constant of $\epsilon_r = 2.43$. Observation was made of the change in input impedance, resonant frequency and the radiation pattern of the microstrip antenna for different positions of reactive loads.

2.2.1 Single loaded microstrip antennas

Extensive experiments were done on microstrip antennas and the results were compared with those evaluated numerically. The experimental results for the microstrip

antenna with single short-circuit loads will be discussed first. The patch size was 6 cm by 4 cm and the antenna was fed at a point (1.0, 1.0) with a co-axial (SMA) connecting probe from the ground plane as is shown in the Figure 1.1. The resonant frequency that was predicted was 2.465 GHz. The variation of input impedance with frequency is shown on Smith charts in Figures 2.2 to 2.5 where the short-circuit load is at a different position on the patch for each case. The magnetic current distribution, which is equivalent to the voltage distribution, was plotted along the patch edges for each of the cases considered using the cavity model. There are four separate plots corresponding to the four edges of the radiator. The positive direction of the axis of these magnetic current plots points away from the patch edge in each case. These distributions are illustrated in Figures 2.2 to 2.5.

The theoretical prediction of the resonant frequency [5], was verified experimentally. The experimental results for input impedance agreed exceptionally well with the theoretically predicted ones in all the cases except for those shown in Figures 2.5. This could be due to experimental error and not due to error in the theoretical model. It was also shown experimentally that if the short circuit load is placed on the locus of points as predicted theoretically by Richards [5] the resonant frequency was almost unchanged. This locus of points is illustrated for the case of a single load in Figure 2.6. The variation of the input impedance as the loads are moved along this locus is illustrated in Figure 2.7. Measurements were also made of the radiation pattern both in the E-plane and the H-plane and for the cross polarized component. These are illustrated in Figures 2.8 to 2.13. An important application of loaded microstrip antennas, as mentioned before, is control of the active impedance of the

array elements as the array is scanned. Switching between these loads can keep the active impedance within reasonable levels of impedance mismatch while at the same time keeping the resonant frequency constant.

2.2.2 Dual loaded microstrip antennas

Similar experiments were performed for the dual-loaded microstrip antennas and the results obtained again agreed well with the theoretically predicted values. Here also the loads were short circuits. The results obtained are illustrated in Figures 2.14 to 2.21. The input impedance of the microstrip antenna could be varied over a wide range with the change in the position of the short circuit load. It was observed that the cross polarized fields were reduced slightly for the dual-loaded case compared to the single-loaded case. The locus of load placement to keep the resonant frequency constant as illustrated in Figure 2.14 was predicted theoretically and was verified experimentally. The variation of the input impedance as the loads are moved along this locus is illustrated in Figure 2.15. As can be seen in the figure, the locus of points where the load can be placed is symmetric about the center line or the nodal line of the unloaded patch.

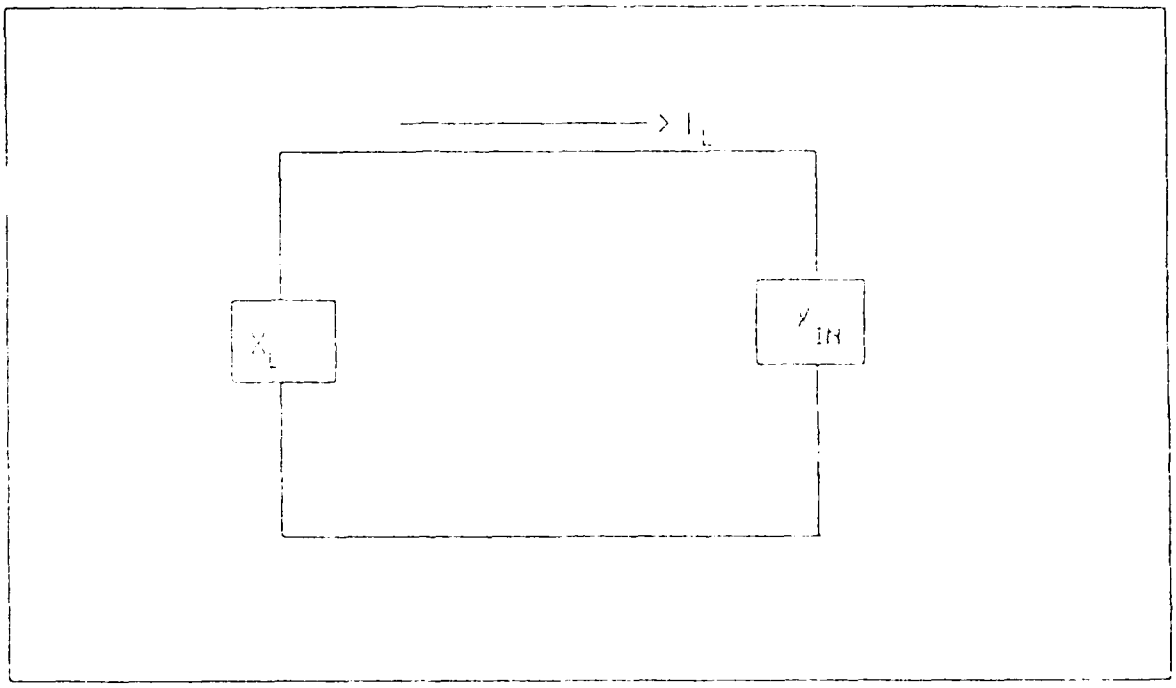

* X_{in} is the input reactance at the load point of an unloaded microstrip cavity

Figure 2.1: The circuit model for the microstrip antenna

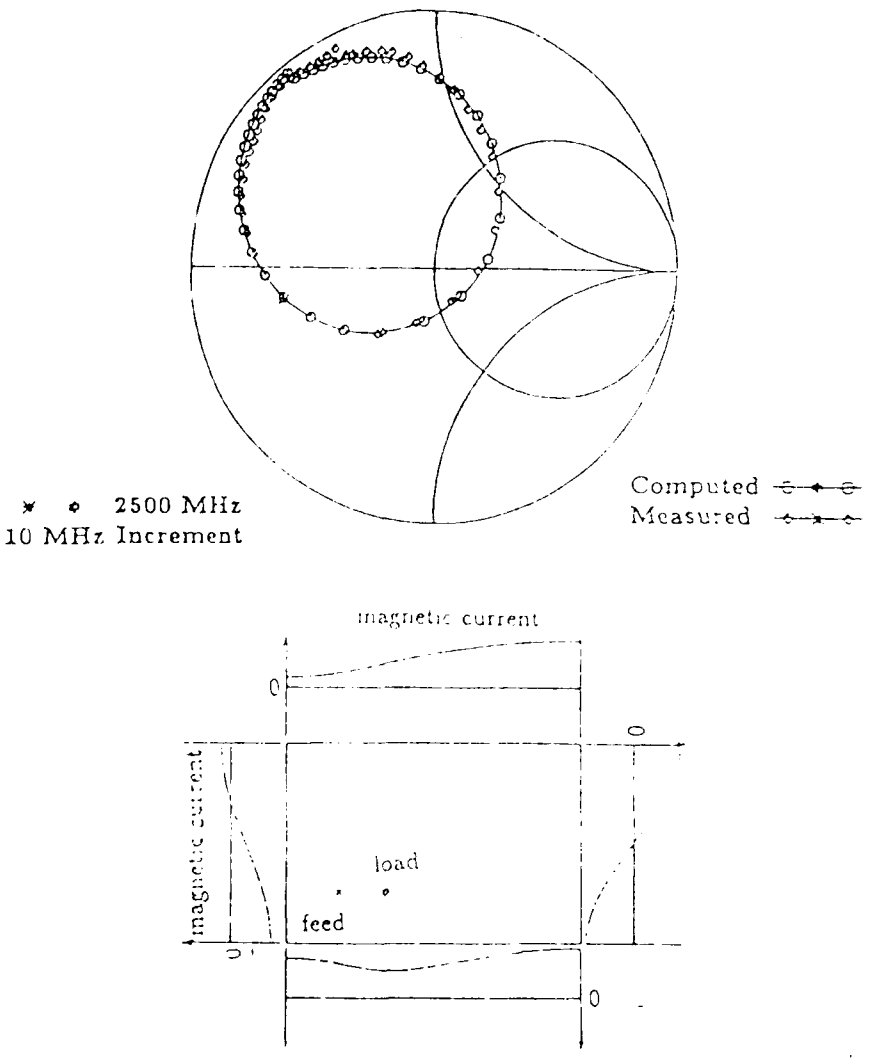

Figure 2.2 The computed and measured input impedance variation and magnetic current distribution of the single loaded microstrip antenna. Patch size 6 × 4 cm , load position (1.75 ,1.04) ; feed position (1,1) ; resonant frequency = 2.465 GHz

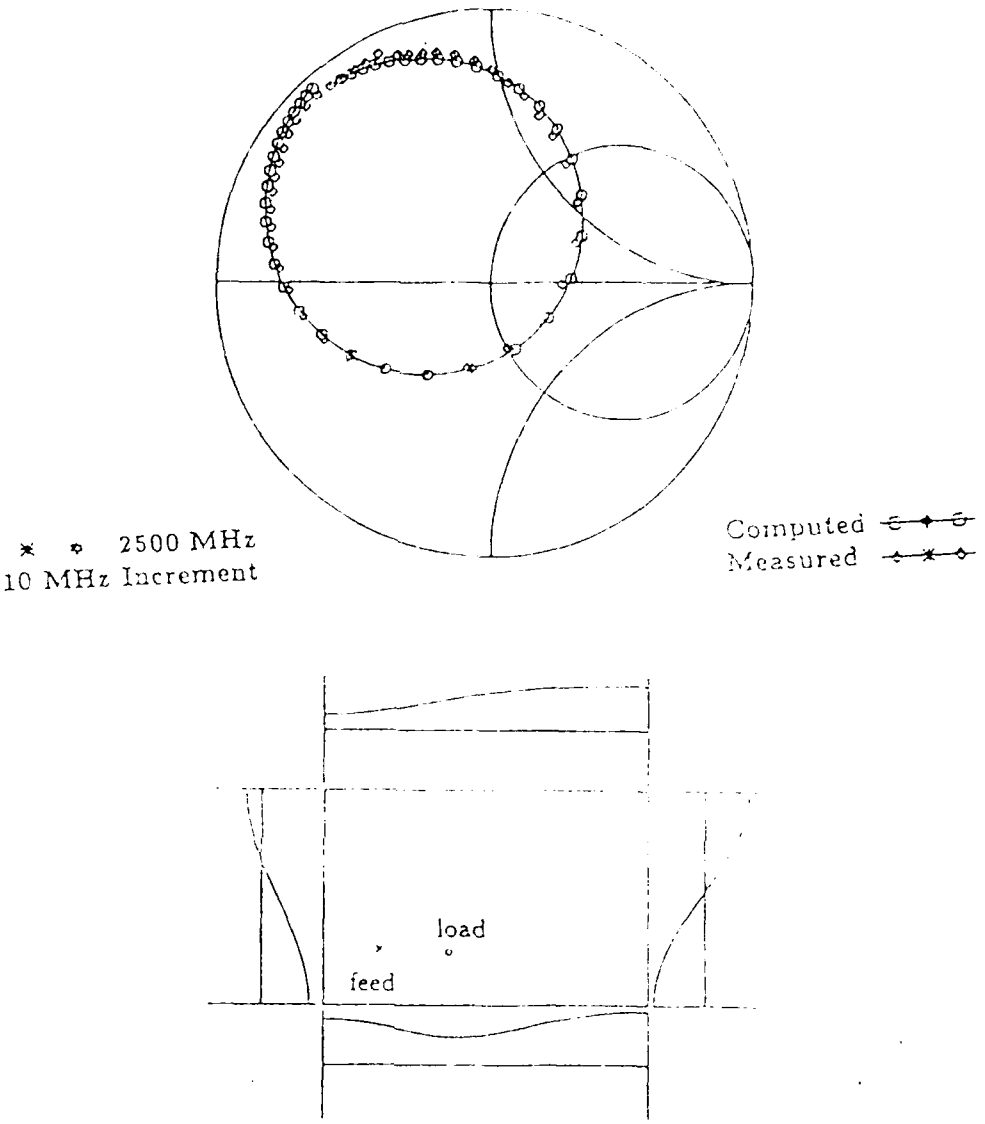

Figure 2.3: The computed and measured input impedance variation and magnetic current distribution of the single loaded microstrip antenna. Patch size 6 × 4 cm , load position (2.25 ,0.95) , feed position (1,1) ; resonant frequency = 2.465 GHz

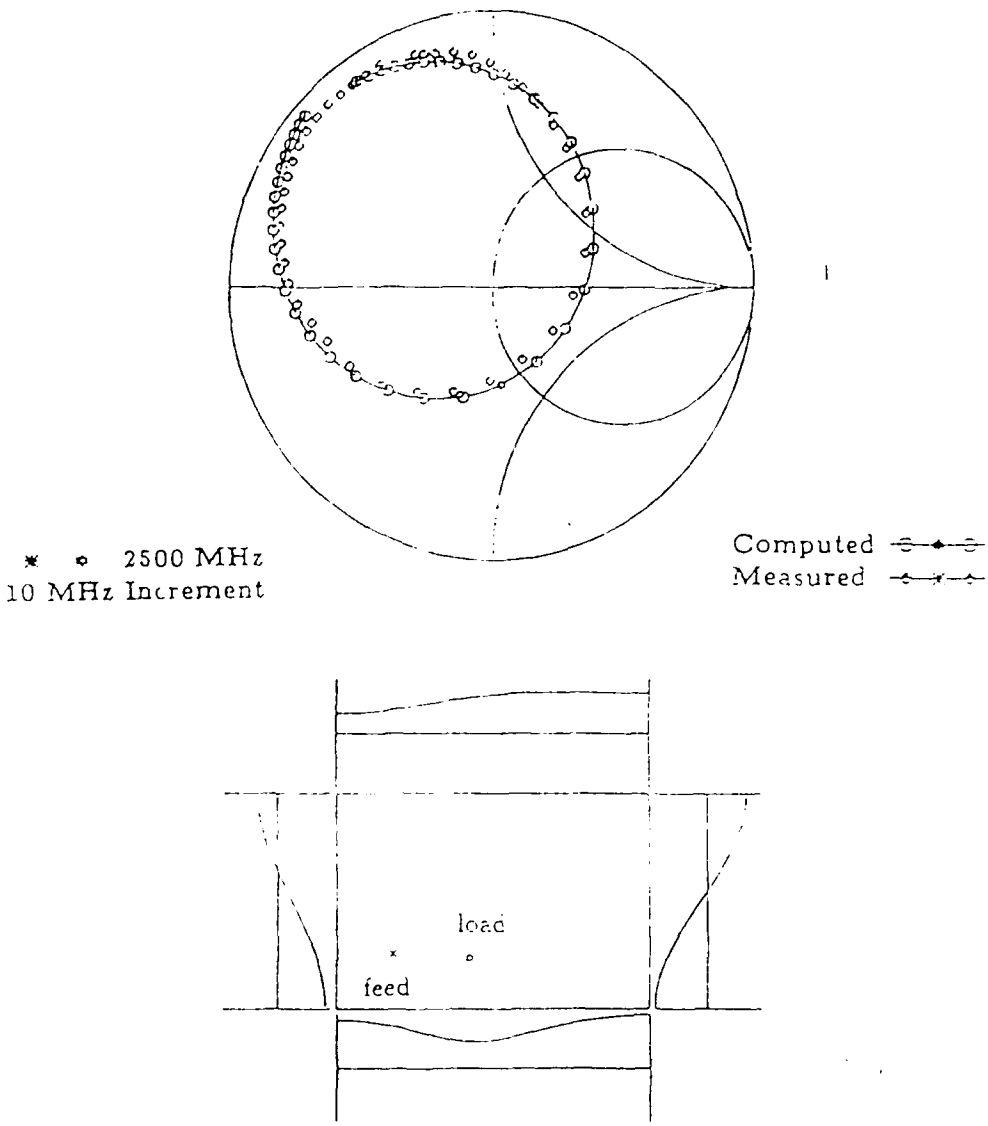

Figure 2.4: The computed and measured input impedance variation and magnetic current distribution of the single loaded microstrip antenna. Patch size 6 × 4 cm. ; load position (2.5 ,0.91) ; feed position (1,1) ; resonant frequency = 2.465 GHz

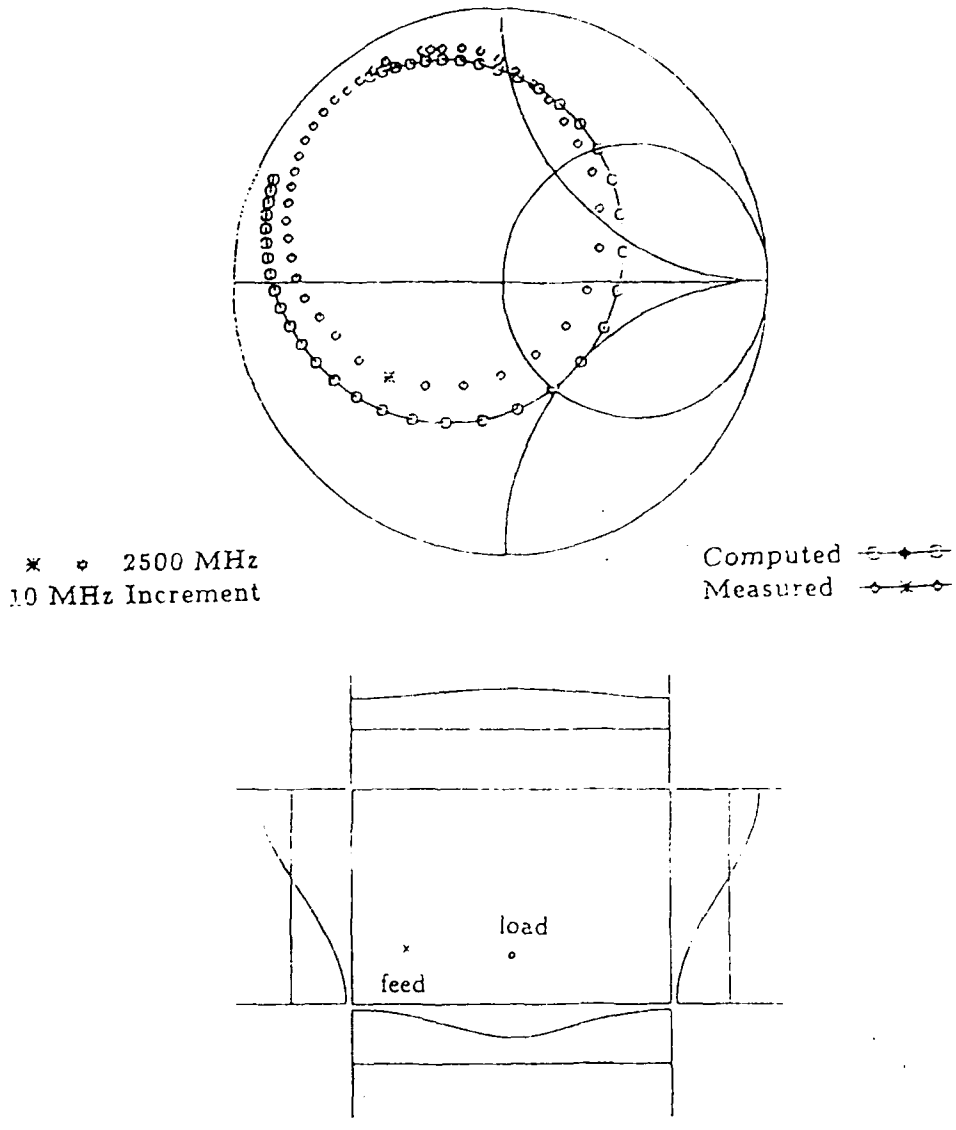

Figure 2.5: The computed and measured input impedance variation and magnetic current distribution of the single loaded microstrip antenna. Patch size 6 x 4 cm ; load position (3.0 ,0.82) ; feed position (1,1) ; resonant frequency = 2.465 GHz

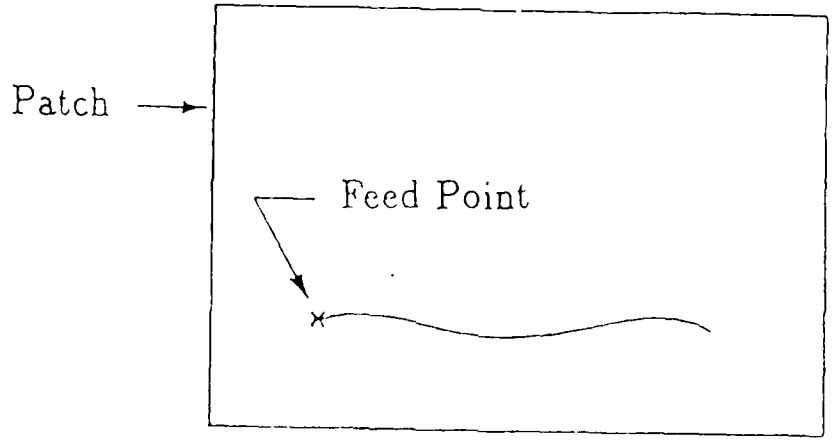

Figure 2.6: Locus of short circuit locations for constant resonant frequency of a single loaded element. Patch size 6 × 4 cm. ; resonant frequency = 2.465 GHz

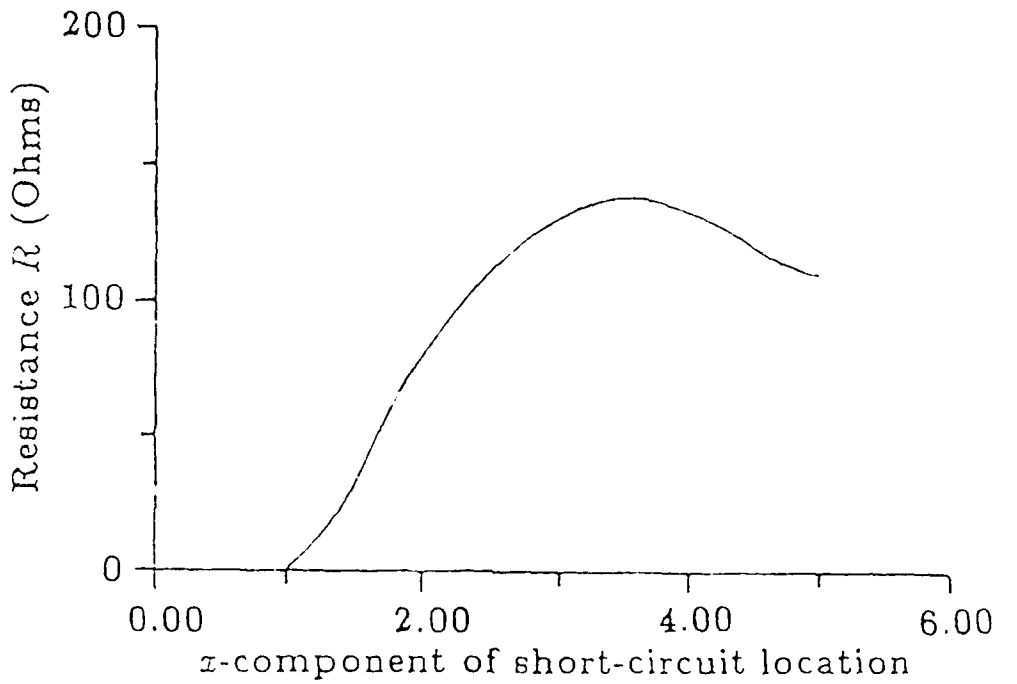

Figure 2.7: The variation of the conductance G with the x-coordinate of a short circuit position taken from the constant resonant frequency locus for a fixed feed at (1,1) ; resonant frequency = 2.465 GHz

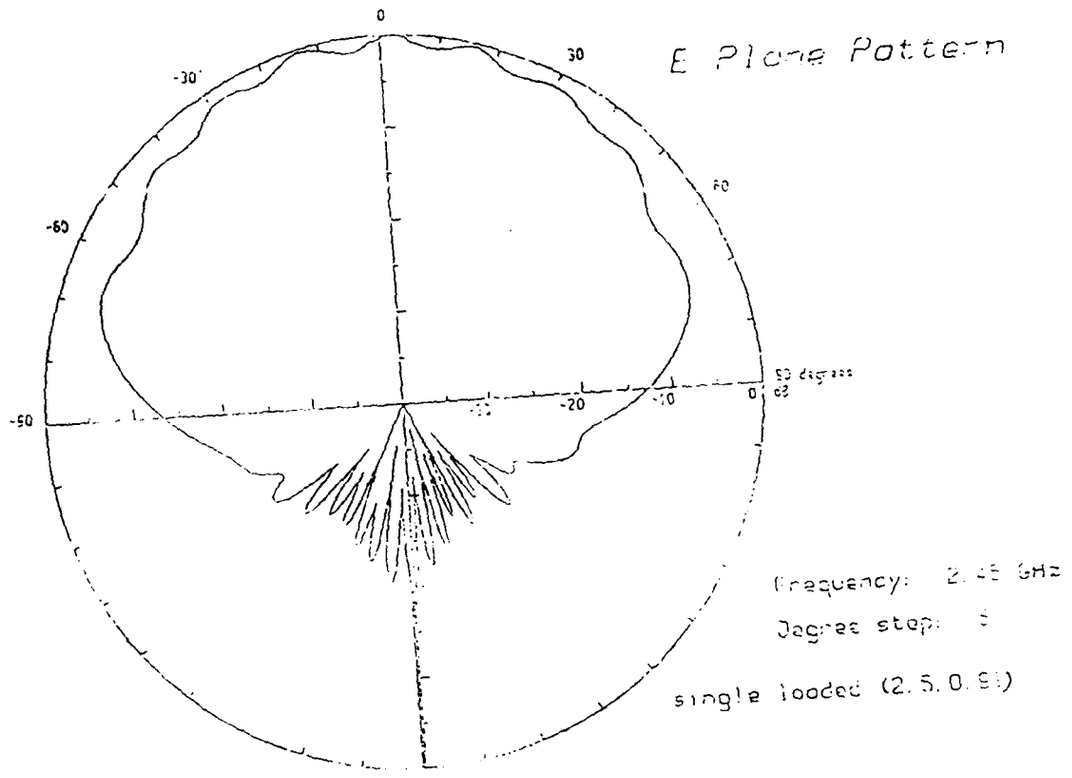

Figure 2.8: The measured E-plane radiation pattern of the single loaded microstrip antenna. (Patch size 6 x 4 cm. ; load position (2.5,0.91) ; feed position (1,1) ; resonant frequency = 2.465 GHz

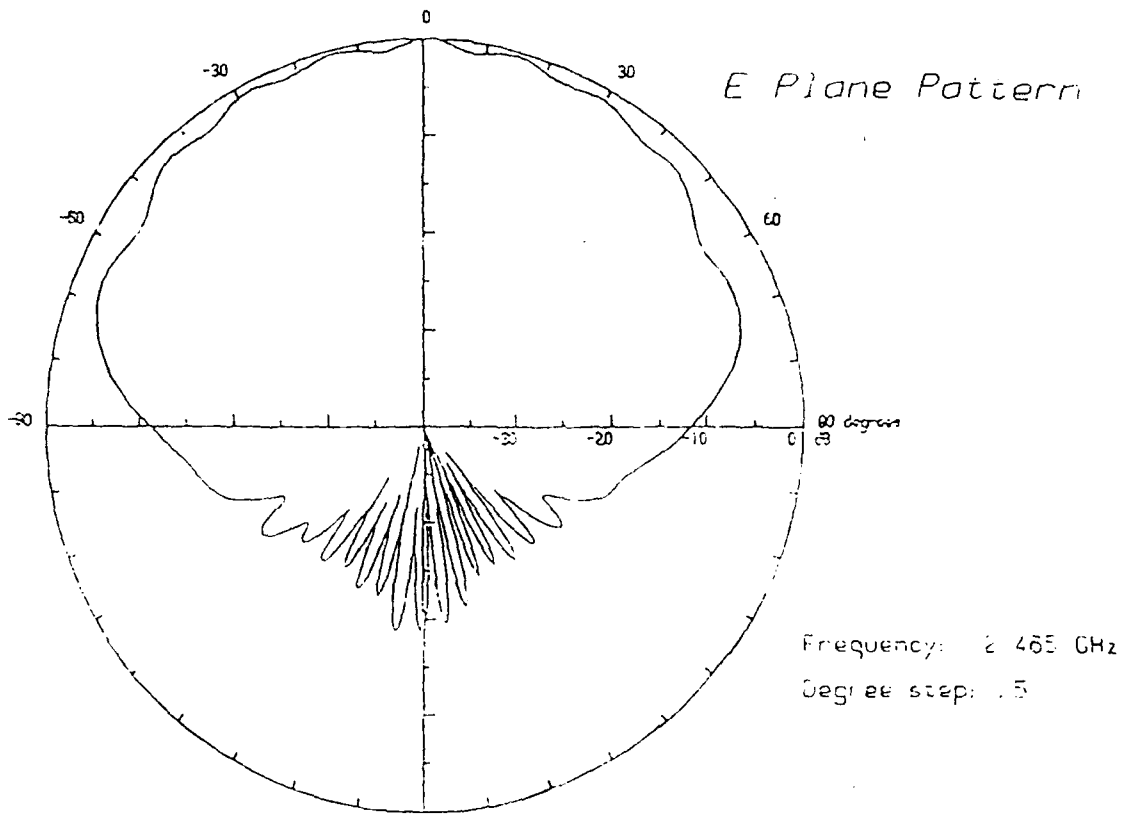

Figure 2.9: The measured E-plane radiation pattern of the single loaded microstrip antenna. (Patch size 6 × 4 cm. ; load position (2.0,1.0) ; feed position (1,1) ; resonant frequency = 2.465 GHz

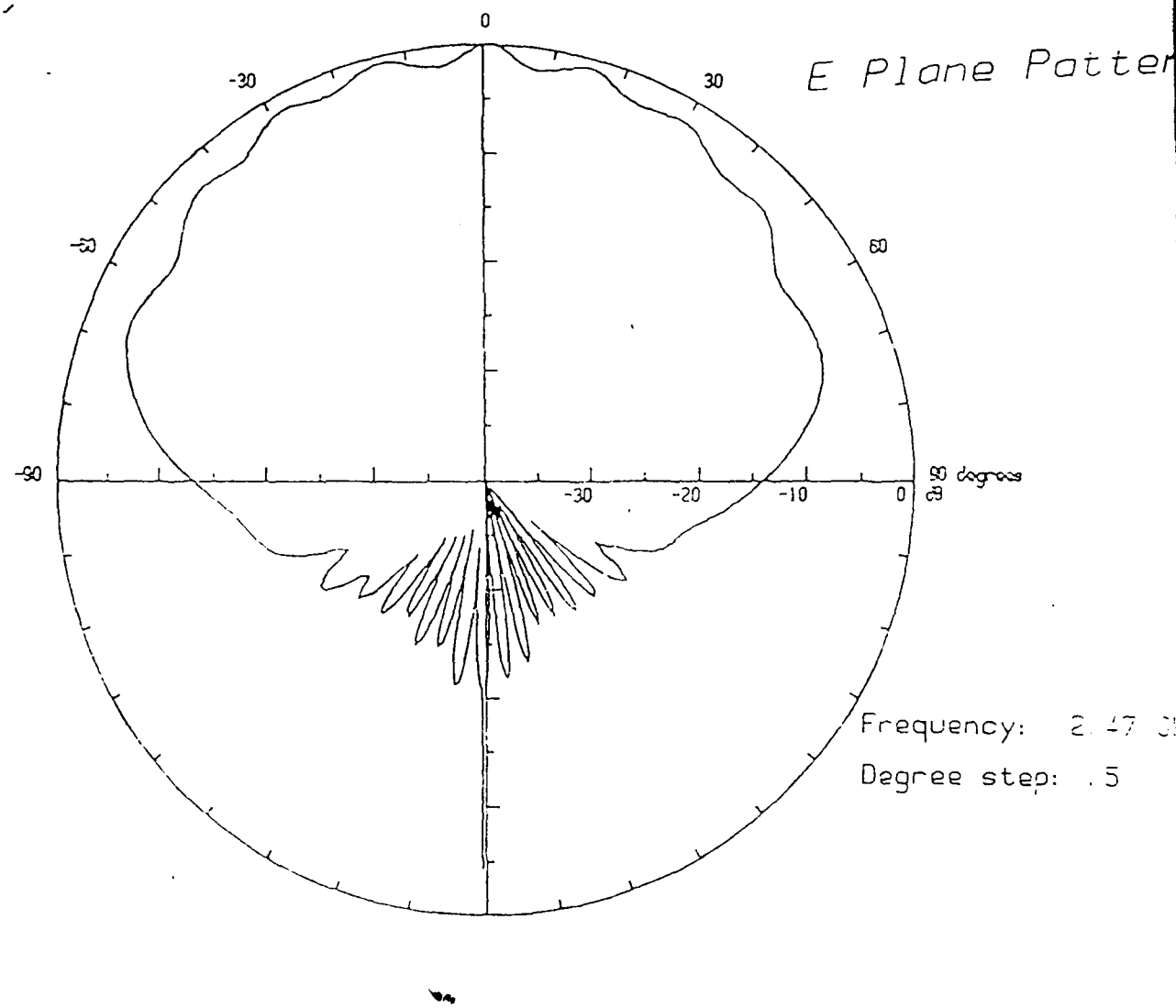

Figure 2.10: The measured E-plane radiation pattern of the single loaded microstrip antenna. (Patch size 6 × 4 cm. ; load position (2.25,0.95) ; feed position (1,1) ; resonant frequency = 2.465 GHz

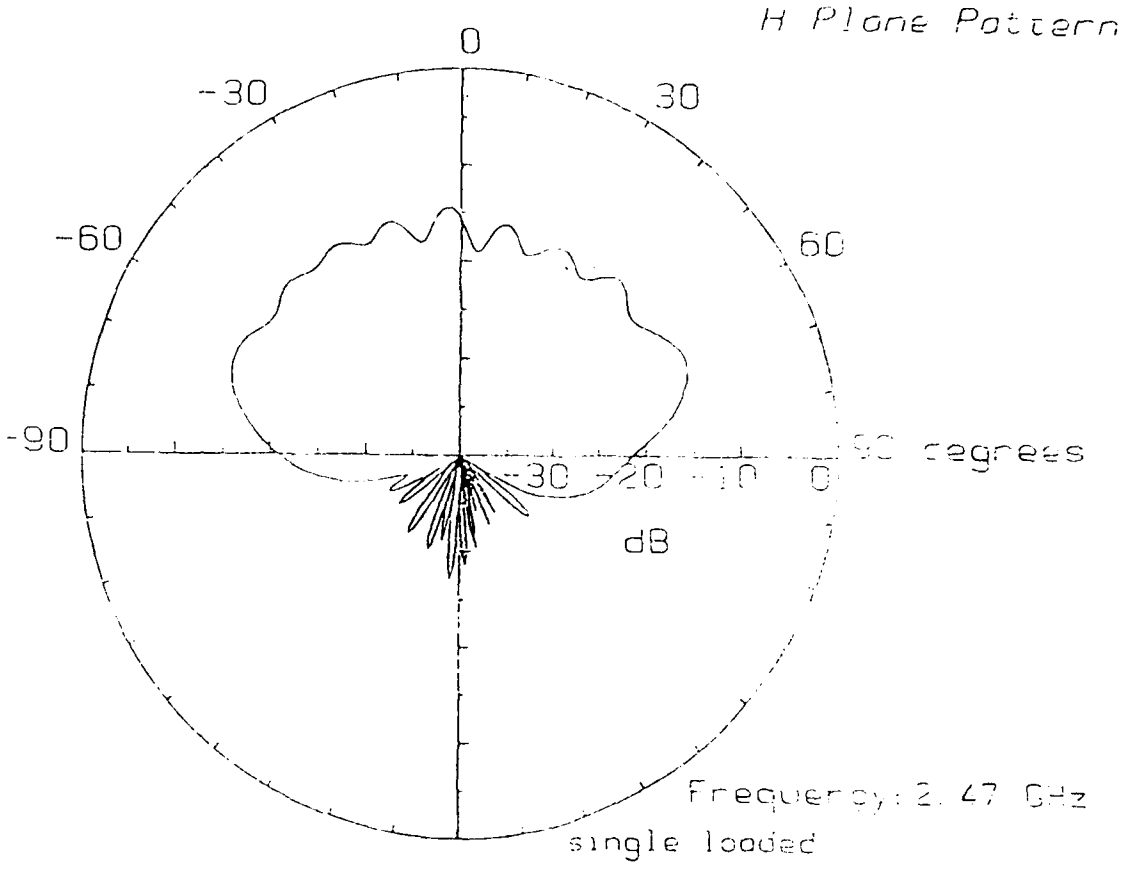

Figure 2.11: The measured H-plane radiation pattern of the single loaded microstrip antenna (patch size 6 x 4 cm.; load position (2.25,0.95) ; feed position (1,1) ; resonant frequency = 2.465 GHz

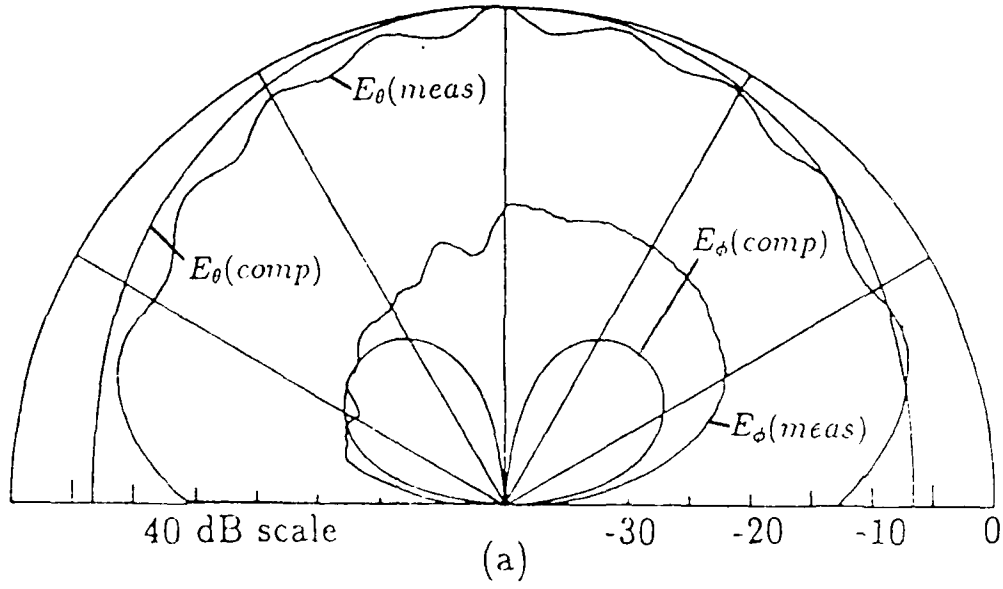

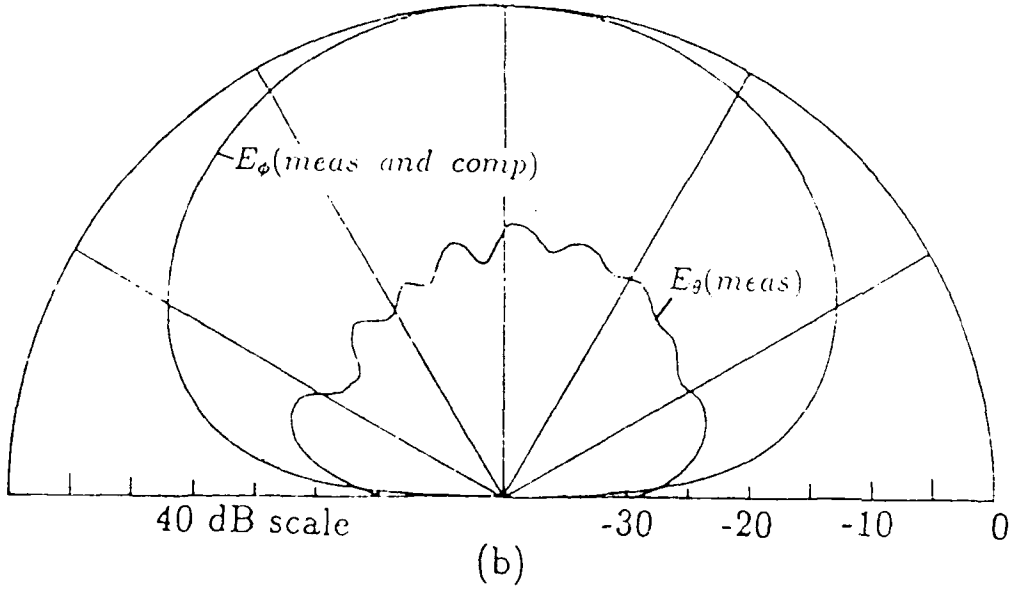

Figure 2.12: (a)The measured and computed input co- and cross-polarised field patterns in the E-plane for short circuit loads at (2.00,1.12) and (2.0,2.88) (b) measured and theoretical patterns in the H-plane (computed E_θ is zero). Resonant frequency = 2.465 GHz

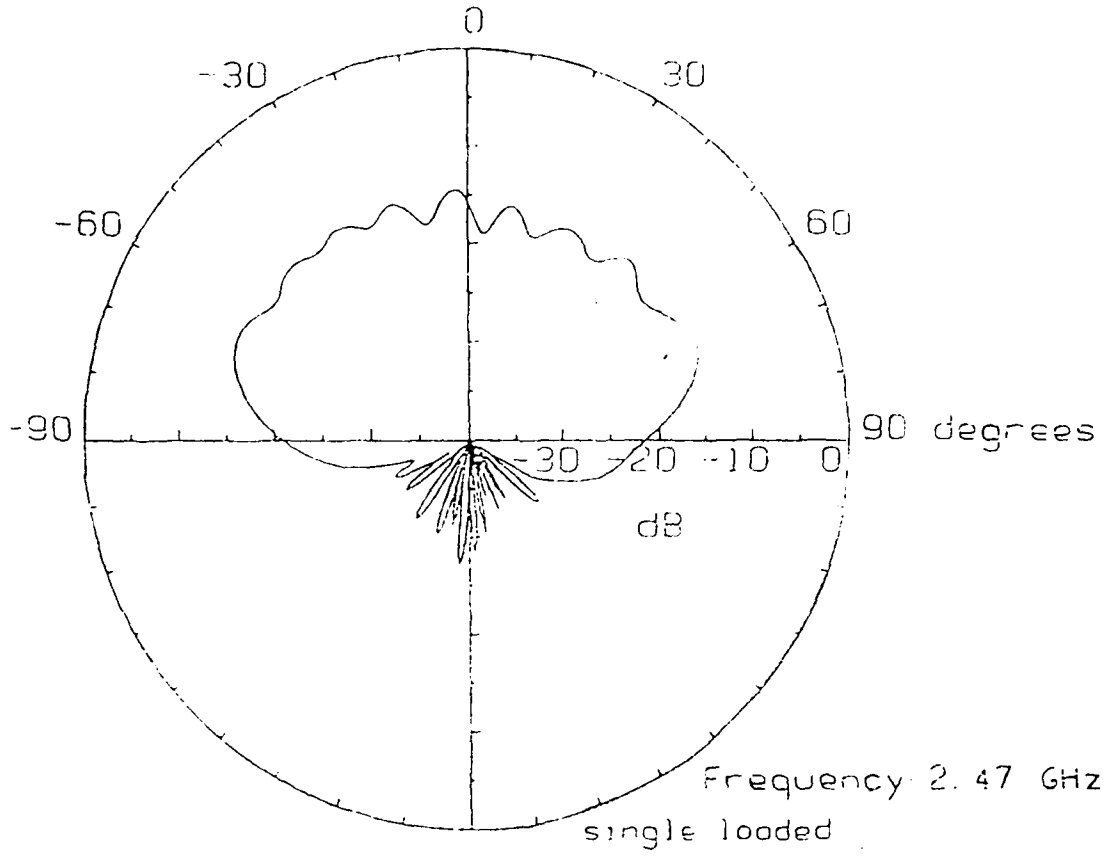

Figure 2.13: The measured H-plane radiation pattern of the single loaded microstrip antenna (patch size 6 × 4 cm.; load position (2.5,0.91) ; feed position (1,1) , resonant frequency = 2.465 GHz

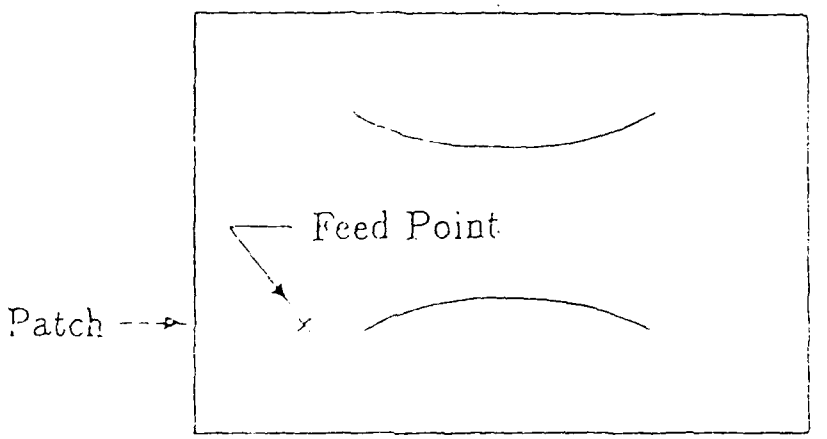

Figure 2.14: Locus of short circuit locations for constant resonant frequency of the double loaded **element**. Patch size 6 × 4 cm. ; resonant frequency = 2.465 GHz

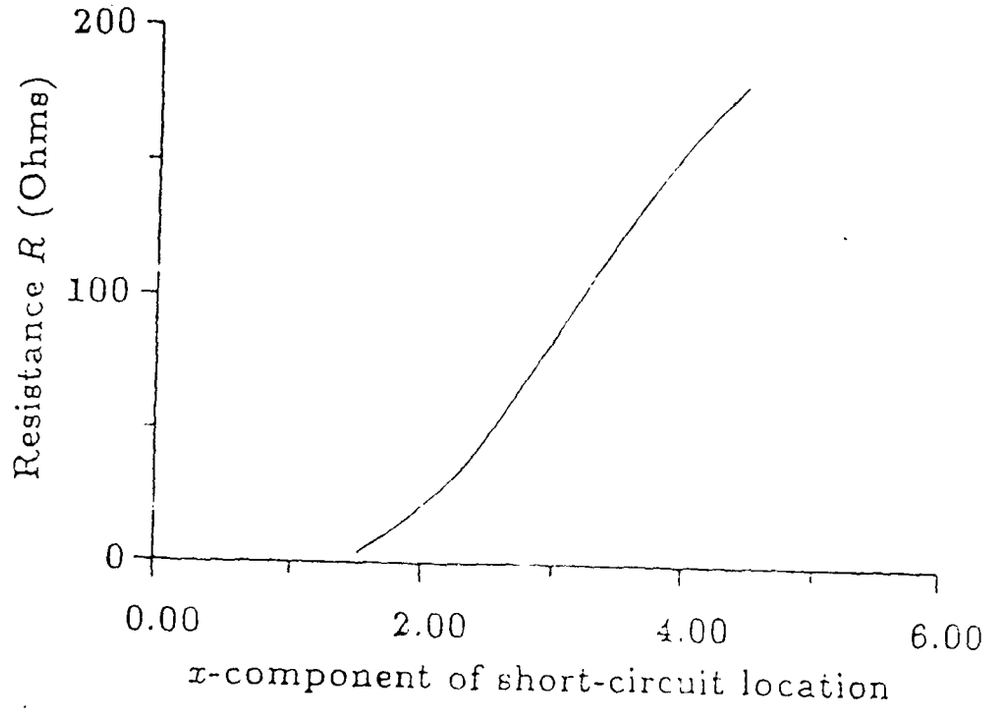

Figure 2.15: The variation of the conductance G with the x-coordinate of a short circuit position taken from the constant resonant frequency locus for a fixed feed at (1,1) ; resonant frequency = 2.465 GHz

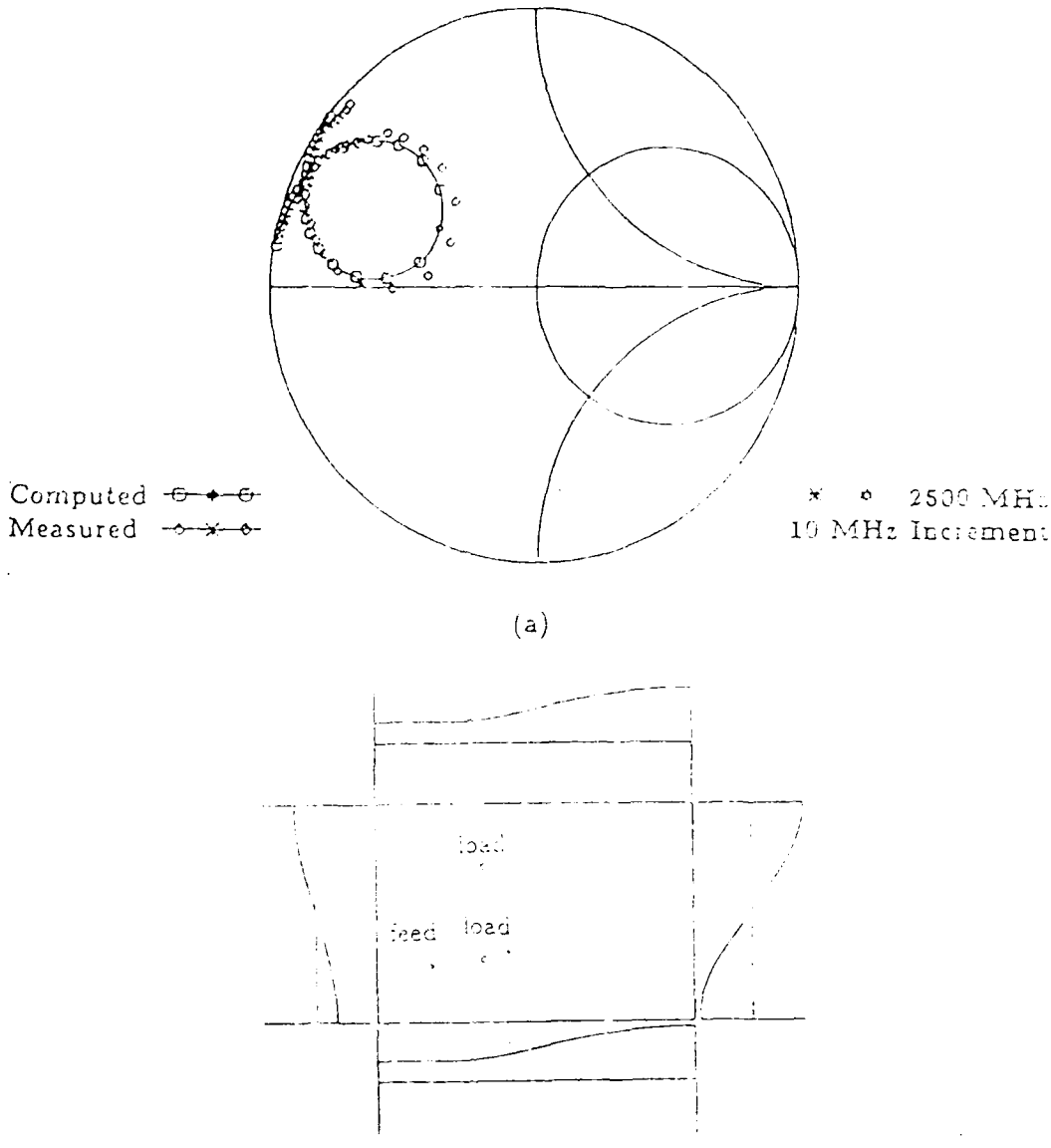

Figure 2.16: The computed and measured input impedance variation of the dual loaded microstrip antenna. (Patch size 6 × 4 cm. , load positions (2 0.1 12) and (2 0.2 88) ; feed position (1,1) ; resonant frequency = 2.465 GHz

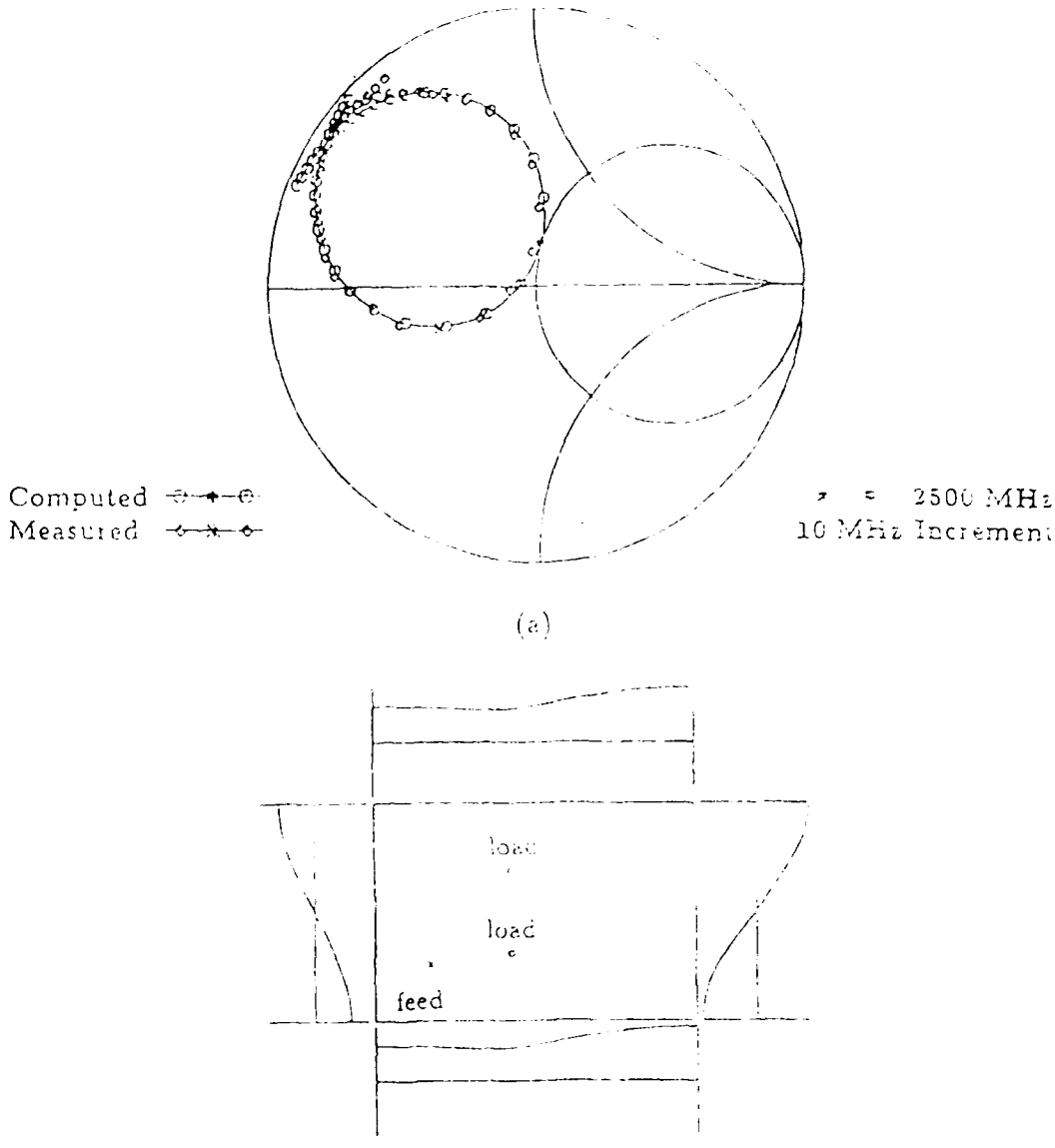

(a)

Figure 2.17: The measured input impedance variation of the dual loaded microstrip antenna. (Patch size 6 x 4 cm. ; load positions (2.5,1.21) and (2.5,2.79) ; feed position (1,1) , resonant frequency = 2.465 GHz

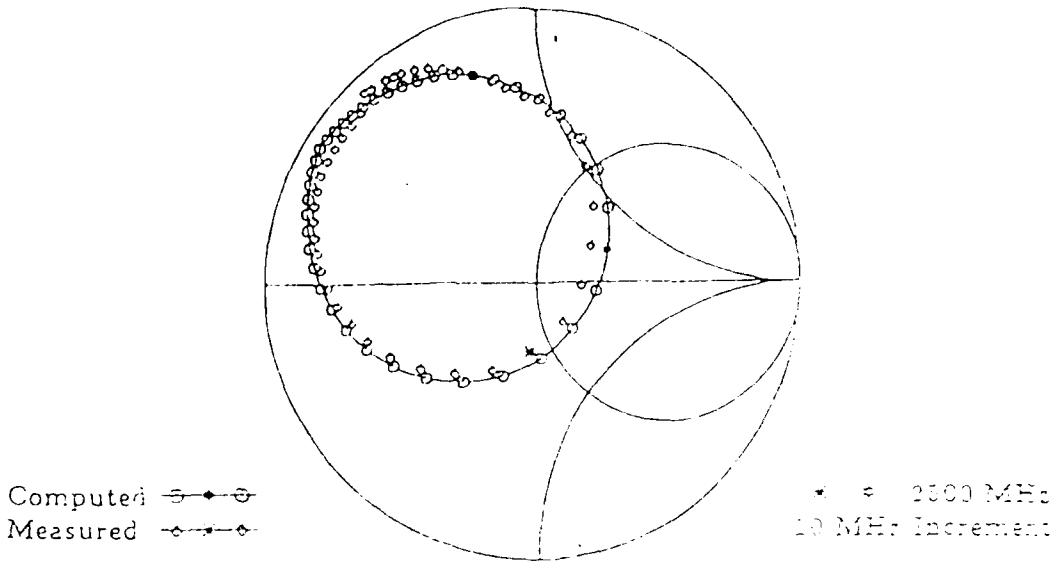

(a)

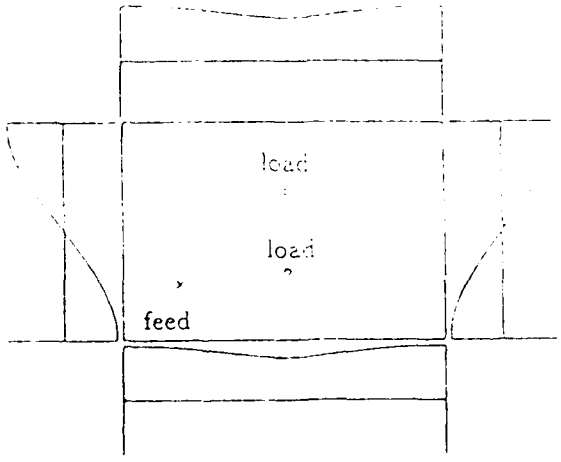

(b)

Figure 2.18 The measured input impedance variation of the dual loaded microstrip antenna (Patch size 6 × 4 cm. , load positions (3.0,1.23) and (3.0,2.77) ; feed position (1,1) ; resonant frequency = 2.465 GHz

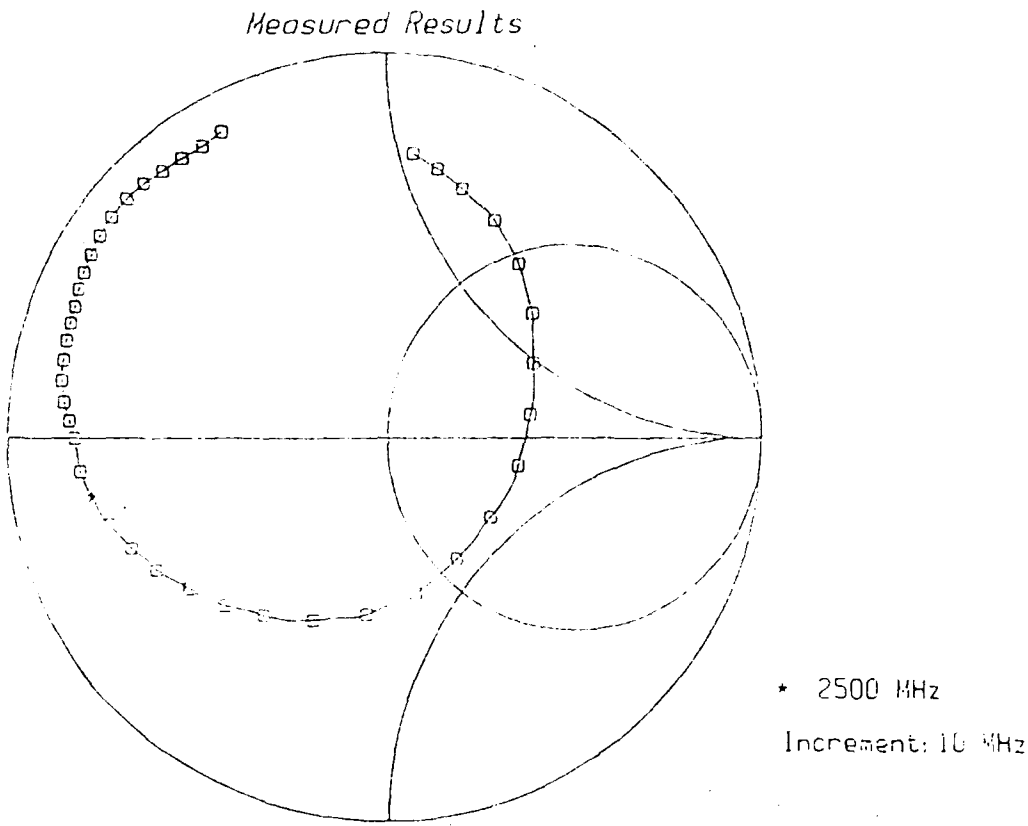

Figure 2.19: The measured input impedance variation of the dual loaded microstrip antenna (Patch size 6 × 4 cm. , load positions (2.0,1.1) and (2.0,2.9) ; feed position (1,1) ; resonant frequency = 2.465 GHz

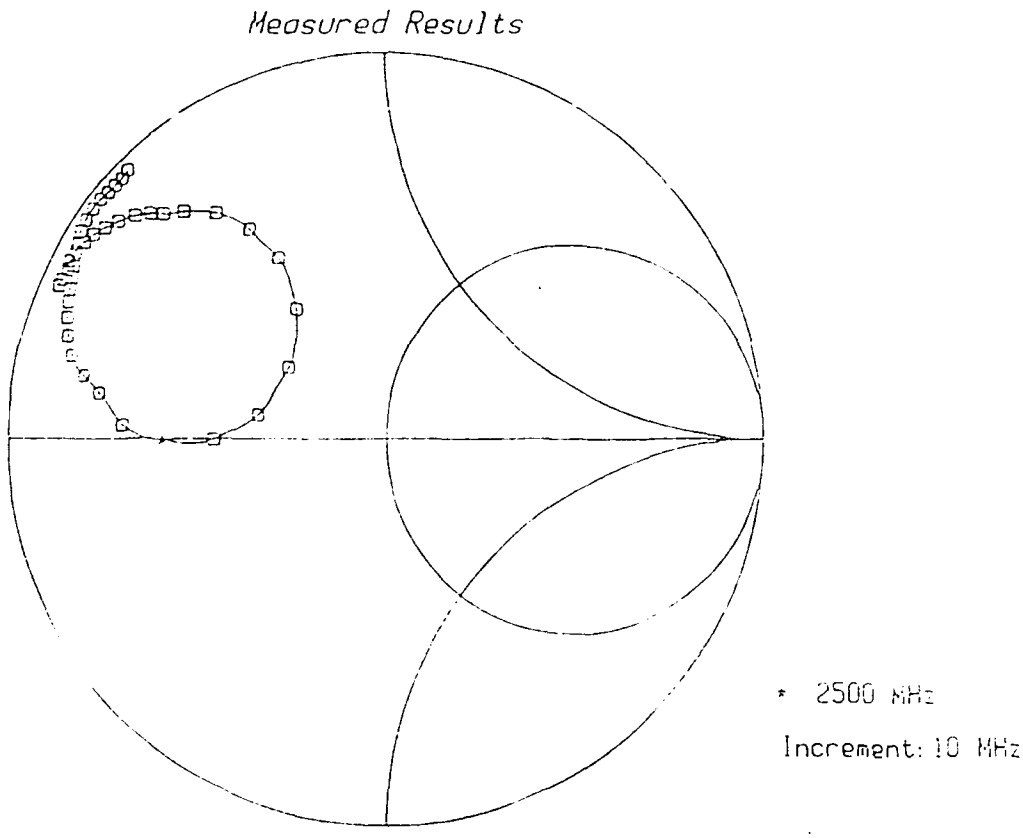

Figure 2.20. The measured input impedance variation of the dual loaded microstrip antenna. (Patch size 6 × 4 cm. ; load positions (2.5,1.21) and (2.5,2.79) ; feed position (1,1) ; resonant frequency = 2.465 GHz

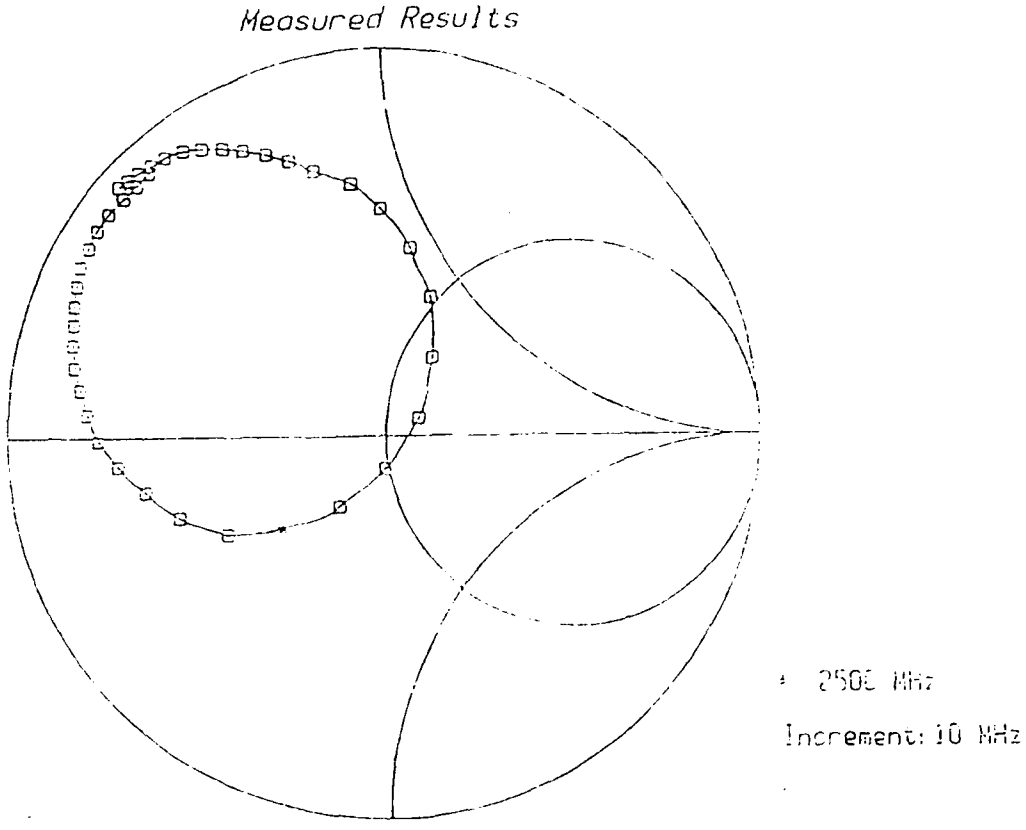

Figure 2.21: The measured input impedance variation of the dual loaded microstrip antenna. (Patch size 6 × 4 cm. , load positions (2.75,1.23) and (2.75,2.77) ; feed position (1,1) ; resonant frequency = 2.465 GHz

Chapter 3

MUTUAL IMPEDANCE BETWEEN MICROSTRIP ANTENNAS

An expression for the mutual impedance between rectangular microstrip patche can be obtained by the use of the reciprocity principle, in particular the Rumse reaction formula, and the use of the formula for the radiation from a unit magneti dipole.

3.1 Radiation from a unit dipole

We shall use an expression for the field from an infinitesimal current element o dipole and then use the duality principle and the reaction formula to develop a expression for the mutual impedance. The expression for the electric field in spher ical coordinates due to a unit dipole in the $\hat{r}$ direction as shown in Figure 3.1 ca be written as [8]

$$\mathbf{E} = \frac{-j\zeta_o}{2\pi k_o}\left(\frac{jk_o}{r^2}+\frac{1}{r^3}\right)e^{-jk_o r}\cos\theta\,\hat{r} + \frac{j\zeta_o}{4\pi k_o}\left(\frac{k_o^2}{r}-\frac{jk_o}{r^2}-\frac{1}{r^3}\right)e^{-jk_o r}\sin\theta\,\hat{\theta} \quad (3.1)$$

where $\hat{\tau}$ is a unit vector in the x-y plane, $k_o = \omega\sqrt{\mu_o\epsilon_o}$ is the wave number or propagation constant in free space and $\zeta_o = (\mu_o/\epsilon_o)^{1/2}$ is the intrinsic impedance of free space. We make use of the duality principle to obtain the expression for the H-field. For this we substitute $1/\zeta_o$ for ζ_o and get the following expression for the H-field

$$\mathbf{H} = \frac{-j}{\zeta_o 2\pi k_o}\left(\frac{jk_o}{r^2} + \frac{1}{r^3}\right)e^{-jk_o r}\cos\theta\,\hat{r} + \frac{j}{4\zeta_o\pi k_o}\left(\frac{k_o^2}{r} - \frac{jk_o}{r^2} - \frac{1}{r^3}\right)e^{-jk_o r}\sin\theta\,\hat{\theta} \quad (3.2)$$

An expression for the H-field can be obtained in rectangular co-ordinates by using the following conversion factors.

$$\hat{r} = \frac{\left((x_j - x_i)\,\hat{x} + (y_j - y_i)\,\hat{y}\right)}{\left((x_j - x_i)^2 + (y_j - y_i)^2\right)^{1/2}} \quad (3.3)$$

$$\hat{\theta} = \frac{(x_j - x_i)\,\hat{y} - (y_j - y_i)\,\hat{x}}{\left((x_j - x_i)^2 + (y_j - y_i)^2\right)^{1/2}} \quad (3.4)$$

$$\vec{r}_x = \frac{(x_j - x_i)\,\hat{x}}{\left((x_j - x_i)^2 + (y_j - y_i)^2\right)^{1/2}} \quad (3.5)$$

$$\vec{r}_y = \frac{(y_j - y_i)\hat{y}}{\left((x_j - x_i)^2 + (y_j - y_i)^2\right)^{1/2}} \quad (3.6)$$

In the above equations the subscript j represents the coordinates at the observation point and the subscript i represents the coordinates at the source point. For the case of the microstrip antennas shown in Figure 3.2 we have the unit tangents along

the x and the y co-ordinates to be

$$\vec{\tau}_x = \frac{\left(x_{(i+1)} - x_i\right)\hat{x}}{\left((x_j - x_i)^2 + (y_j - y_i)^2\right)^{1/2}} \tag{3.7}$$

$$\vec{\tau}_y = \frac{\left(y_{(i+1)} - y_i\right)\hat{y}}{\left((x_j - x_i)^2 + (y_j - y_i)^2\right)^{1/2}} \tag{3.8}$$

Using these unit tangents, the cosine of the angle θ shown in Figure 3.2 can be represented as

$$\cos\theta = \vec{\tau}_x \cdot \vec{\tau}_x + \vec{\tau}_y \cdot \vec{\tau}_y \tag{3.9}$$

3.2 Mutual impedance using reciprocity principles

The reciprocity principle is used in electromagnetics and especially in antenna theory in deriving the relations between the receiving and transmitting properties of an antenna. Consider Figure 3.3 where a volume V is bounded by a surface S containing two sets of a-c sources, J_a, M_a and J_b, M_b. Using Maxwell's equations and the divergence theorem we can easily derive an expression relating the fields and the currents on the two surfaces. We denote the electric and magnetic fields produced by source a to be E_a and H_a and that produced by the source b to be E_b and H_b respectively. The reaction concept for the fields of source a on source b and vice versa can be stated as

$$< a, b > = < b, a > \tag{3.10}$$

where

$$< \mathrm{a}, \mathrm{b} >= \int\int\int (E_{\mathrm{a}} \cdot J_{\mathrm{b}} - H_{\mathrm{a}} \cdot M_{\mathrm{b}}) dv \tag{3.11}$$

Equation 3.10 can be rewritten as

$$\int\int\int (E_{\mathrm{a}} \cdot J_{\mathrm{b}} - H_{\mathrm{a}} \cdot M_{\mathrm{b}}) dv = \int\int\int (E_{\mathrm{b}} \cdot J_{\mathrm{a}} - H_{\mathrm{b}} \cdot M_{\mathrm{a}}) dv \tag{3.12}$$

For the case of the two microstrip antennas of Figure 3.2, M_{b} and J_{a} are zero. Therefore the mutual impedance can be expressed as

$$Z_{\mathrm{ab}} = \frac{1}{I_{\mathrm{a}} I_{\mathrm{b}}} \oint_S H_{\mathrm{b}} \cdot M_{\mathrm{a}} dS \tag{3.13}$$

where I_{a} and I_{b} are the feeding currents of antennas **a** and **b**.

The magnetic current distribution around the microstrip patch is obtained by using the cavity model [5]. The magnetic current values are obtained at discreet points along the patch edges. The expression for the H field due to the radiation from an infinitesimally small magnetic current source is used in the above expression for computing the mutual impedance between any two microstrip antennas. The currents I_{a} and I_{b} are assumed to be unity in the numerical evaluation of the above integral. The samples of magnetic currents along the patch edges are considered as infinitesimal current sources and the contribution of all such sources is used to compute the mutual impedance.

In practice, at microwave frequencies the scattering parameters $[S]$ are generally used rather than the impedance parameters. Applying the well-known matrix relation [9]

$$[S] = ([Z] - [I])([Z] + [I])^{-1} \tag{3.14}$$

an $n \times n$ $[Z]$ matrix is converted to an $[S]$ matrix of the same order. Here since $n = 2$, $S_{11} = S_{22}$ and $S_{12} = S_{21}$, the equation for S_{21} is

$$S_{21} = 2\tilde{Z_{21}}/((\tilde{Z_{11}} + 1)^2 - \tilde{Z_{21}^2} \tag{3.15}$$

where $\tilde{Z_{11}}$ and $\tilde{Z_{21}}$ are the normalized self impedance, and mutual impedance respectively.

3.3 Application to arrays

The computation of the mutual impedance in an array with more than two elements can be done by using the same procedure as above. In this case mutual coupling between each pair of elements must be calculated. A linear array of microstrip antennas is illustrated in Figure 3.4. Here the mutual impedance can be calculated by taking into account the mutual coupling due to all individual elements. This can be generalized for the case of a planar array which is illustrated in Figure 3.5. The relation between the voltages and the currents flowing in the microstrip antennas, which can be modelled as loads, is illustrated in matrix form as shown below

$$\begin{pmatrix} V_1 \\ V_2 \\ \vdots \\ V_n \end{pmatrix} = \begin{pmatrix} Z_{11}Z_{12}\cdots\cdots Z_{1N} \\ Z_{21}Z_{22}\cdots\cdots Z_{2N} \\ \vdots\vdots\vdots \\ Z_{N1}Z_{N2}\cdots\cdots Z_{NN} \end{pmatrix} \begin{pmatrix} I_1 \\ I_2 \\ \vdots \\ I_N \end{pmatrix}$$

Therefore, we can write the equations relating the voltage and currents as

$$V_1 = Z_{11}I_1 + Z_{12}I_2 + \cdots + Z_{1N}I_N \tag{3.16}$$

Assuming $I_N = 1 \cdot e^{j\phi_N}$ where ϕ_N is a specified phase shift angle, one obtains the expression

$$Z_{\text{active}} = Z_{11} + Z_{12}.e^{j(\phi_2 - \phi_1)} + \cdots + Z_{1N}.e^{j(\phi_N - \phi_1)} \tag{3.17}$$

In the above expression Z_{1N} can be calculated using equation 3.13 and therefore, we can calculate the active impedance of every element in either a linear array or a planar array. As stated earlier the input impedance of loaded microstrip antennas can be varied by reactive loading while keeping the resonant frequency and pattern constant. As the array is scanned the varying active impedance of the array elements produce an impedance mismatch which can possibly be minimized by loading the microstrip antenna elements and switching the loads accordingly as the array is scanned. The performance of the array may thus be improved. This is considered in the next chapter.

3.4 Computed and measured results

3.4.1 Computed results

A Fortran program was written by the author to evaluate the mutual impedance effects in a rectangular patch array. The program enables one to simulate the array on the basis of the model developed previously in Section 3.2 and to compute the active impedance of each element of a linear array with any patch size, edge to edge separation, resonant frequency, number of sample points considered along the edges where the magnetic currents have been computed, and any progressive phase shift angle. The run time of the program depends on the number of sample points of magnetic currents used in the computations. The program can be used for both the E-plane and the H-plane scan. Here the plane perpendicular to the patch and parallel to the electric field is called the E-plane, and that parallel to the magnetic field is called the H-plane. The magnetic current samples were obtained by using the cavity model. These magnetic current samples are evaluated at the resonant frequency found from the program written by Dr. W. F. Richards of the Department of Electrical Engineering of the University of Houston. The two programs have been integrated together for the purpose of obtaining these computed results.

The various computed results are shown in the figures that follow. The variation of the magnitude of mutual coupling was computed as a function of distance between the patches. This is shown in Figure 3.6 for varying distance in the H-plane. In Figure 3.7 we see the variation of mutual coupling with distance in the E-plane. The change in mutual coupling with distance is observed to be less for the E-plane case than for the H-plane. The mutual coupling is represented in Figures 3.8 and 3.9 in

decibels. The results obtained are approximate due to the approximate model used for their computation. It may be stated here that for the purpose of examining the feasibility of the use of loaded elements in an array for improved performance, the approximate model is sufficient.

3.4.2 Mutual impedance measurements

Extensive experiments were performed to measure the mutual impedance between antenna patches with varying separation. The patches were made on printed circuit board manufactured by 3M having a substrate of relative permittivity $\epsilon_r = 2.45$ and substrate thickness of 0.152 cm. The patches were fed with a coaxial SMA connector. All measurements were made on the HP 8510 network analyzer with an absorbing chamber around the antenna. The frequency was varied from 1.65 to 3.15 GHz. Some of the results that were obtained are represented in the Figures 3.10 to 3.19. In the case where there are more than two patches present in an array the effect of an open-circuited patch on the mutual coupling of any other two patches was studied. It was found that this effect was more pronounced in the H-plane than in the E-plane. A possible explanation for this could be the effect of surface waves being more predominant in the H-plane than in the E-plane. Figures 3.10 and 3.11 illustrate this effect which contributes to the error in computation of mutual impedance using the classical reaction formula. A correction to this is proposed in the paper to be published [10] by D.R. Jackson, W.F. Richards and the author.

3.4.3 Mutual coupling for loaded patches

Measurements done for loaded patches are shown in Figures 3.20 to 3.28. In these experiments two patches were studied in a linear array environment both in the E-plane and in the H-plane. The HP 8510 network analyzer was used to make all measurements. It was noted that significant error was introduced in all the mutual coupling measurements from the reflections from the roof and other objects in the laboratory. Therefore an absorbing chamber was made around the antenna and measurements taken were then found to be very repeatable. The loads, as in the previous cases of individual loaded antennas, were short circuits. The position of the load was found to be critical in order to keep the resonant frequency unchanged. Measurements were made for both single and double loads. The load position on one patch was fixed and the load on the second patch was moved along the locus (to keep the resonant frequency constant) and the effect on mutual coupling and the active input impedance of both the patches was studied. It can be seen from these results that the mutual coupling and also the active input impedance of the patches can be varied with changes in load positioning.

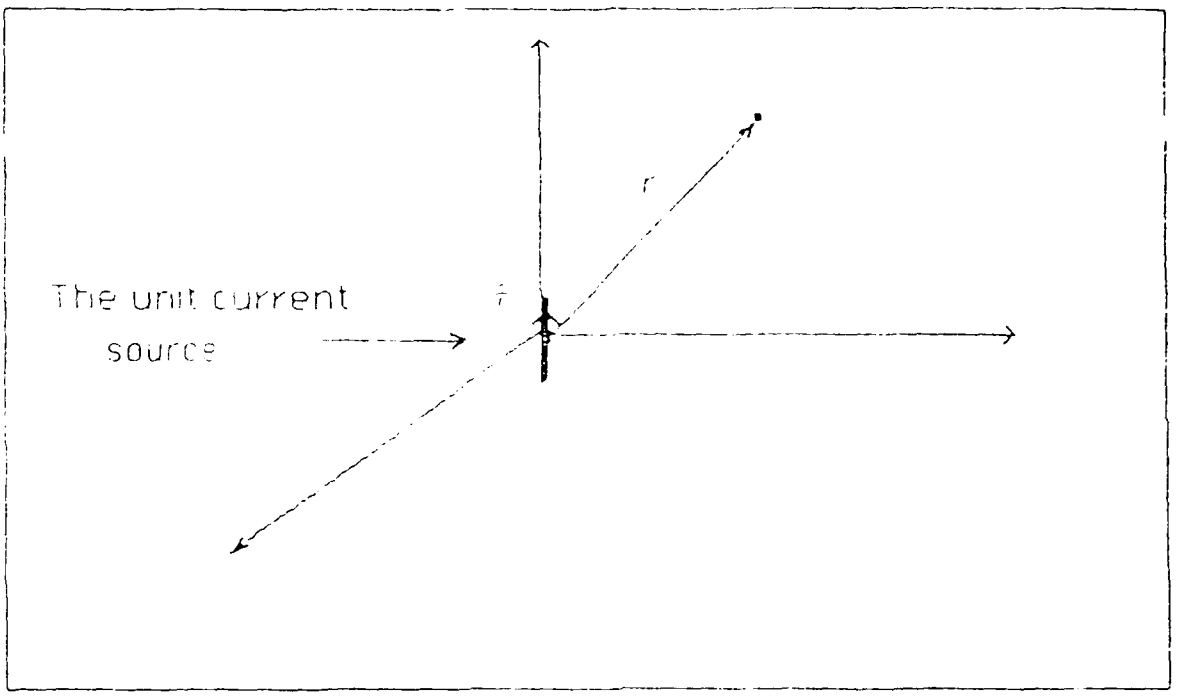

Figure 3.1. The unit current source co-ordinate system used for derivation of the fields

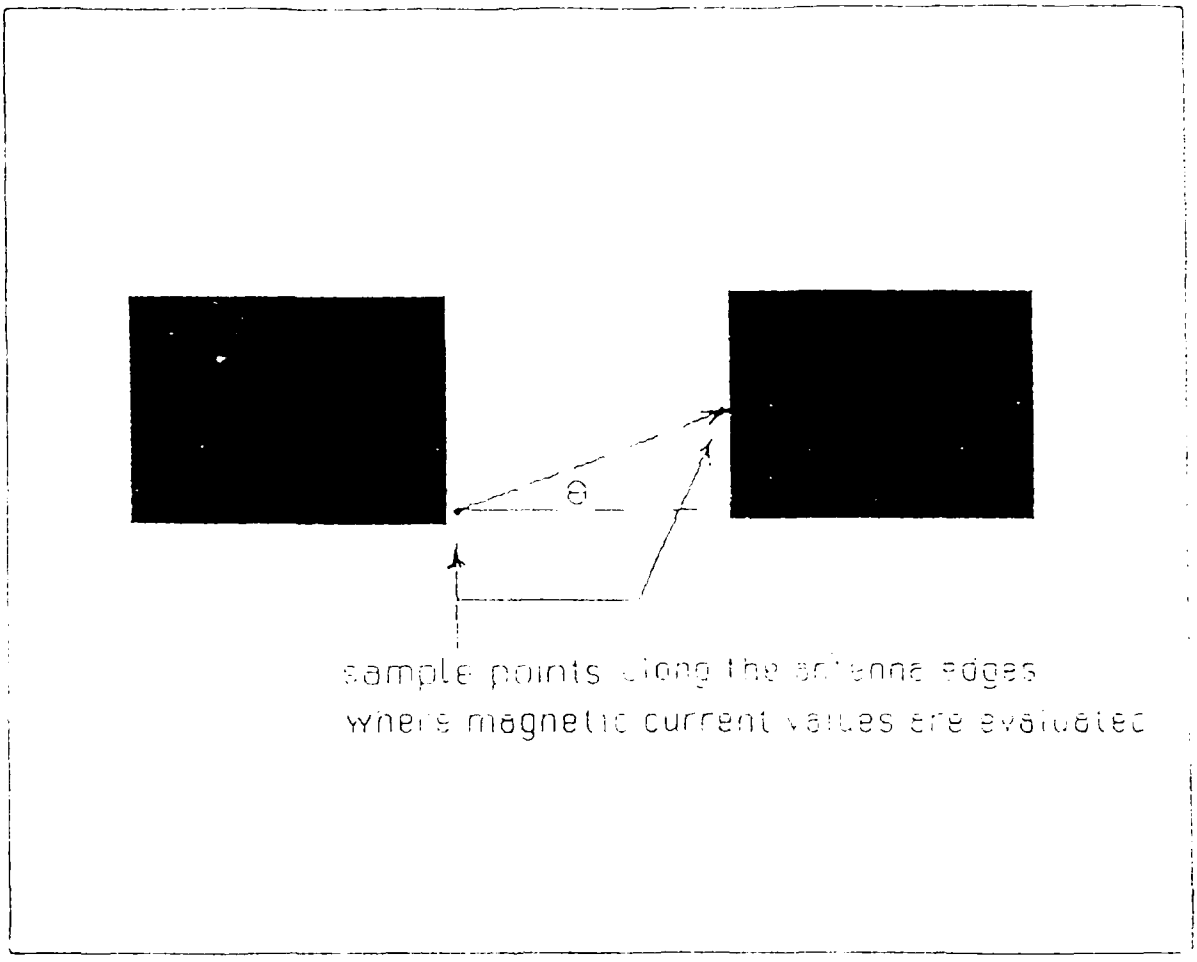

Figure 3.2: The source and the observed microstrip antennas showing the angle θ between sample points along the antenna edges

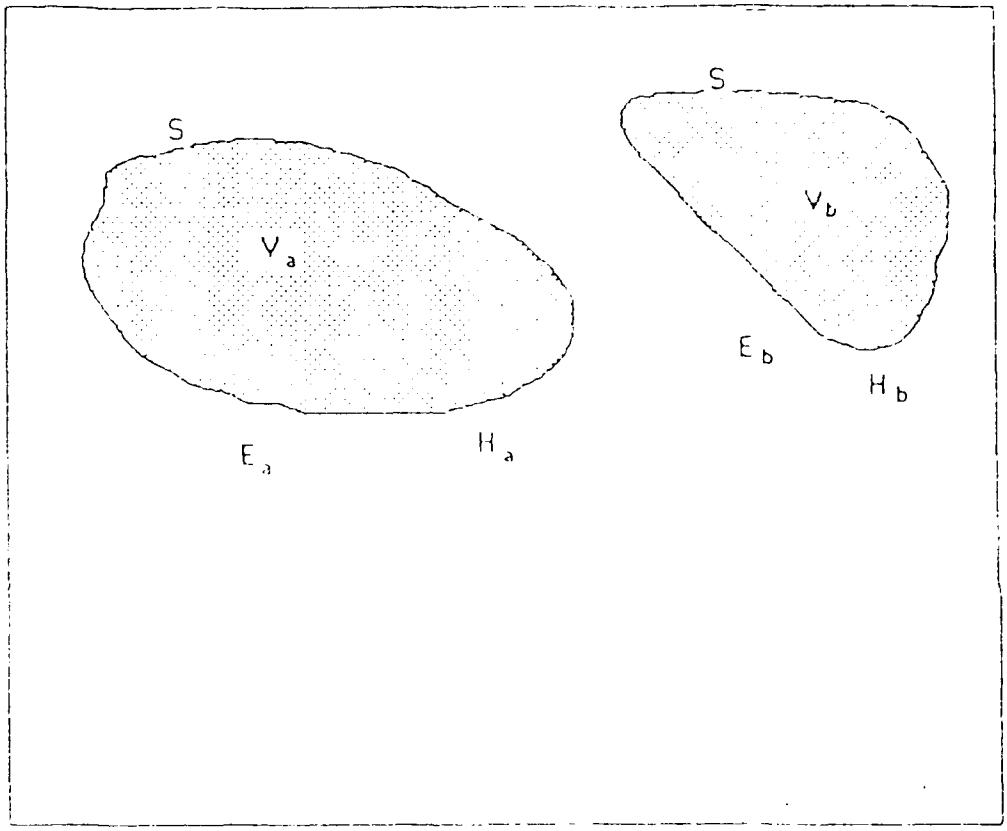

Figure 3.3: The illustration of the reciprocity principle using the bounded volumes

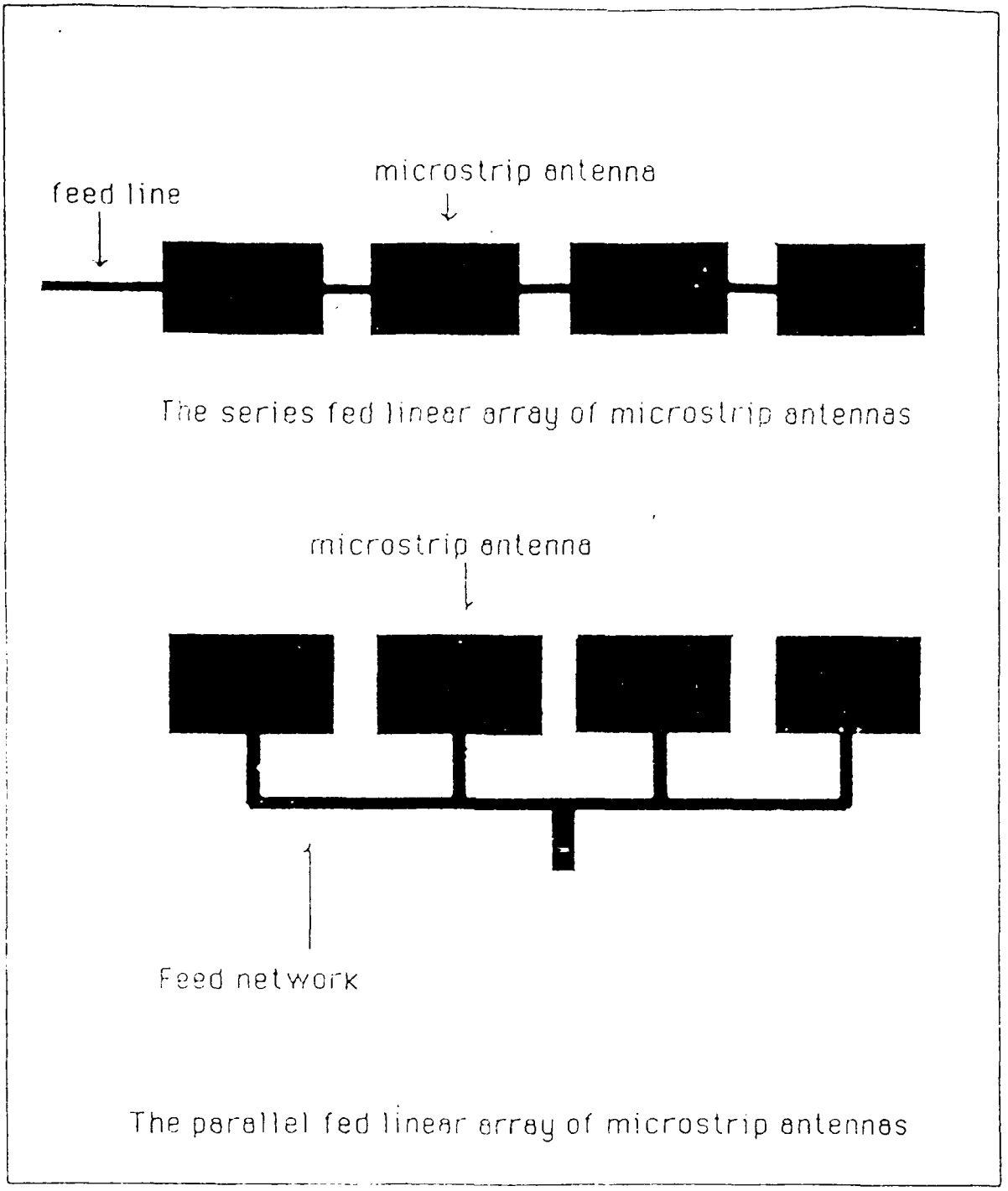

Figure 3.4 The linear array of microstrip antennas showing different feed configurations

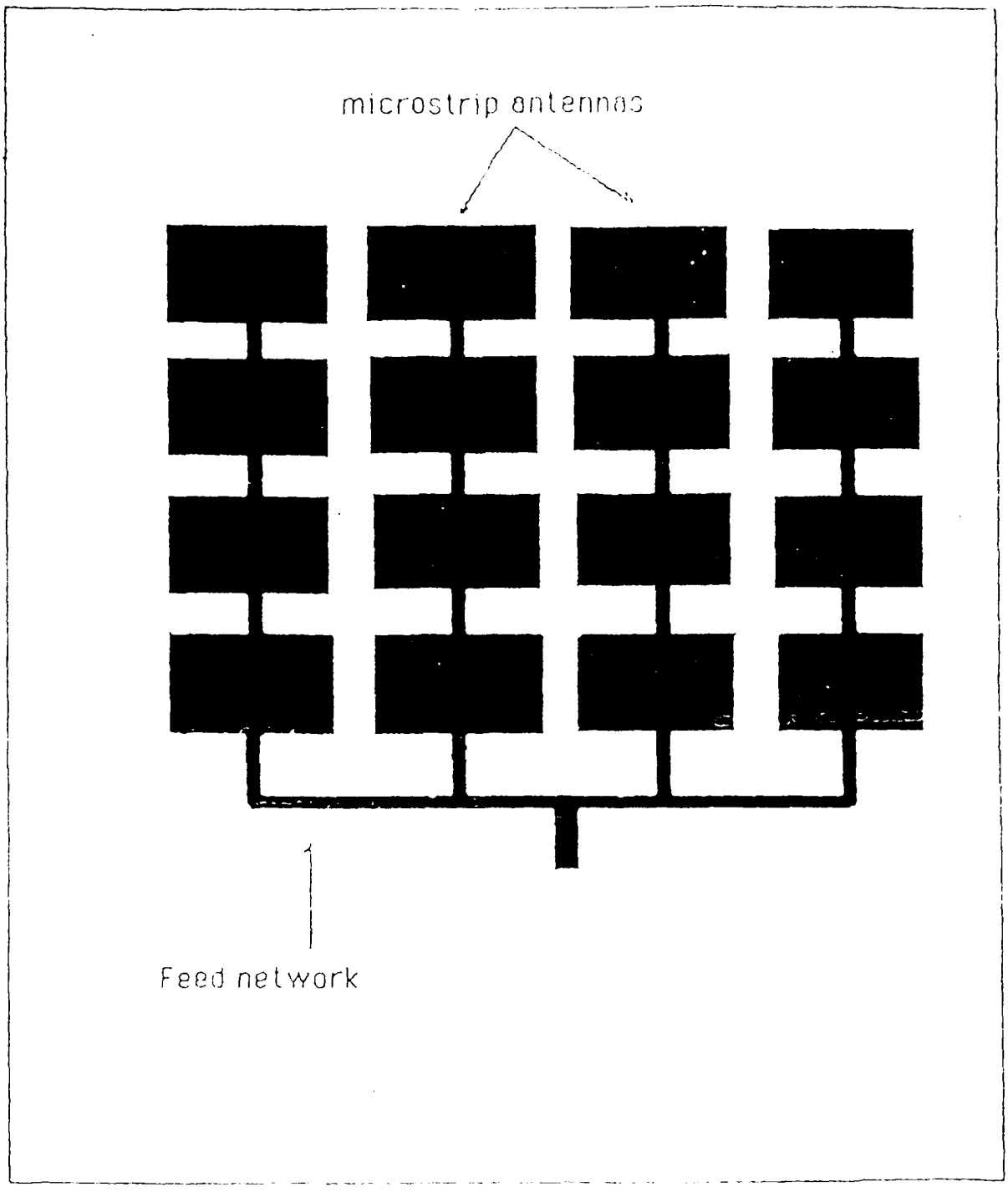

Figure 3.5: The planar array in a simple feed configuration of serial and parallel fed radiators

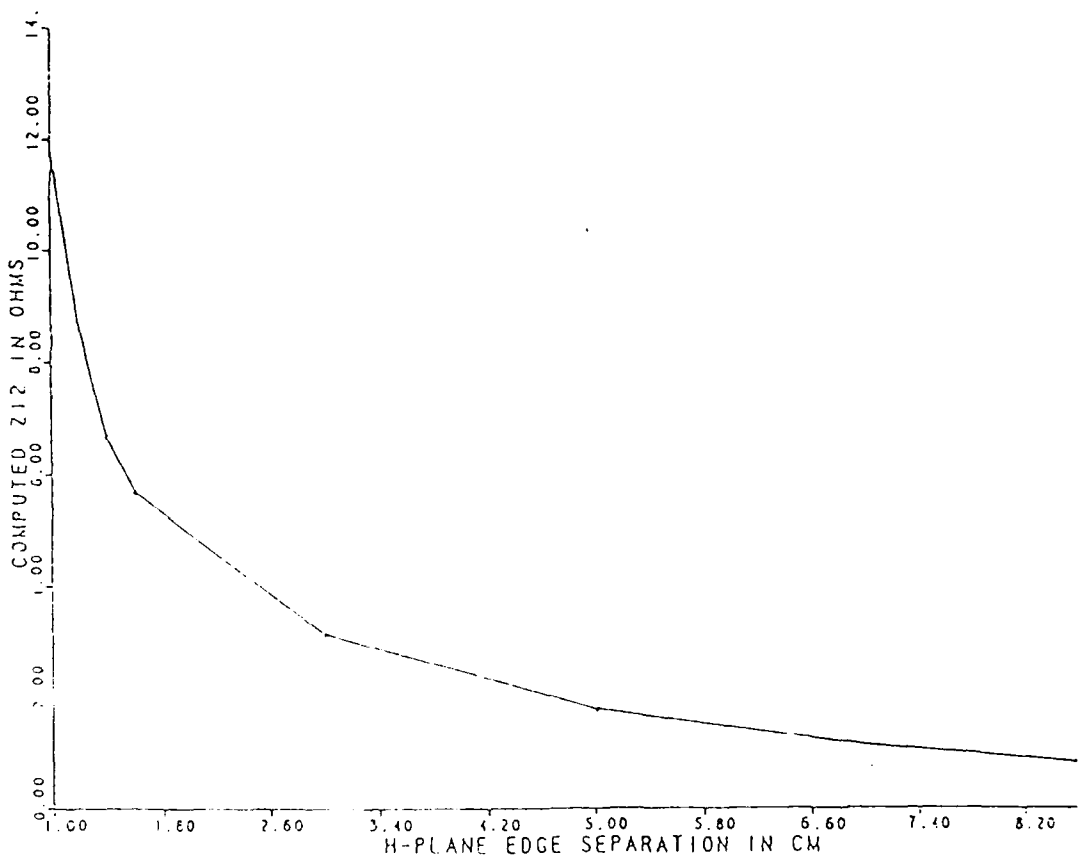

Figure 3.6: The computed variation of the mutual impedance between two microstrip antennas (size 6 × 4 cm ; frequency = 2.35 GHz ; $\epsilon_r = 2.45$) as a function of distance in the H-plane

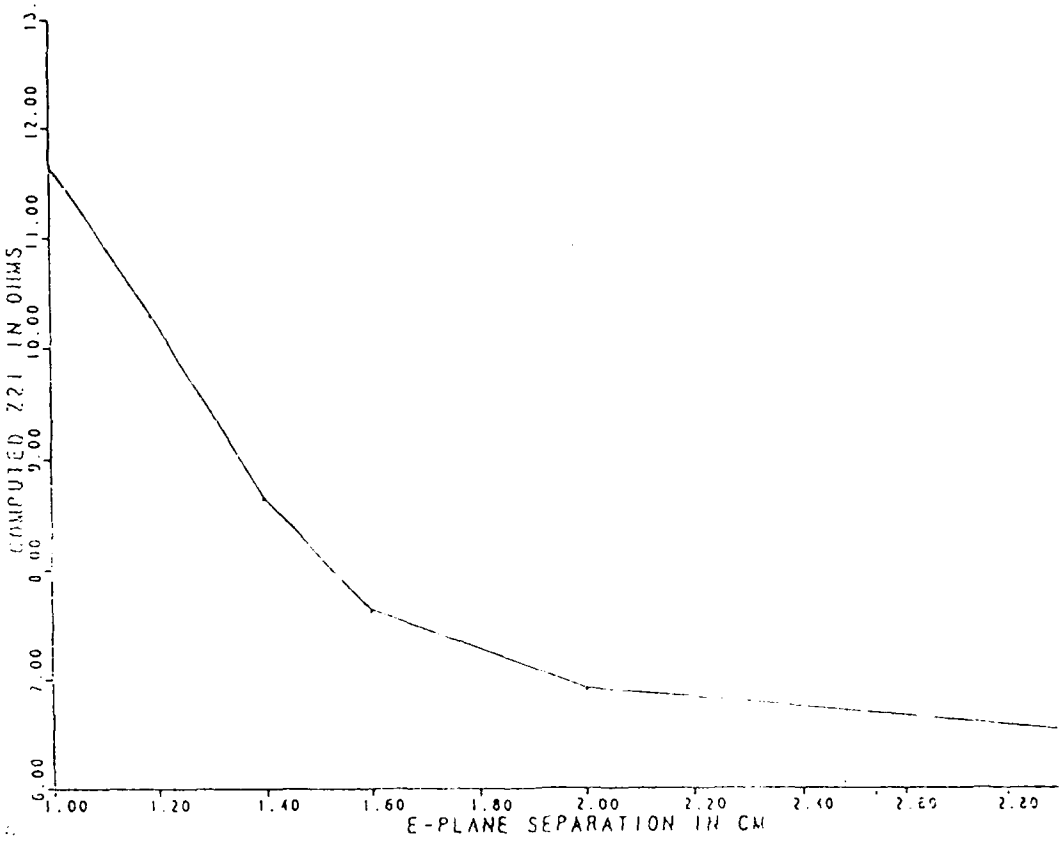

Figure 3.7: The computed variation of the mutual impedance between two microstrip antennas (size 6 × 4 cm ; frequency =2.35 GHz ; $\epsilon_r = 2.45$) as a function of distance in the E-plane

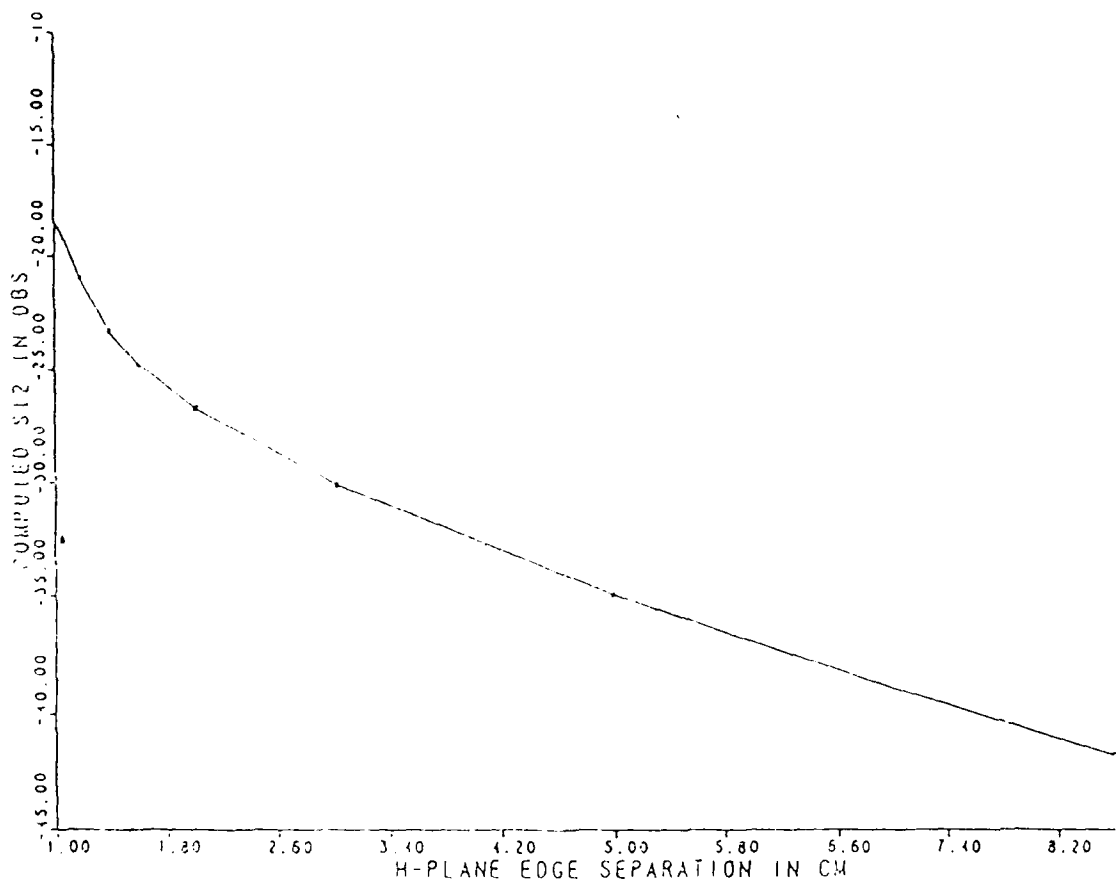

Figure 3.8: The S_{12} representation of the computed variation of the mutual impedance between two microstrip antennas (size 6 × 4 cm ; frequency = 2.35 GHz) as a function of distance in the H-plane

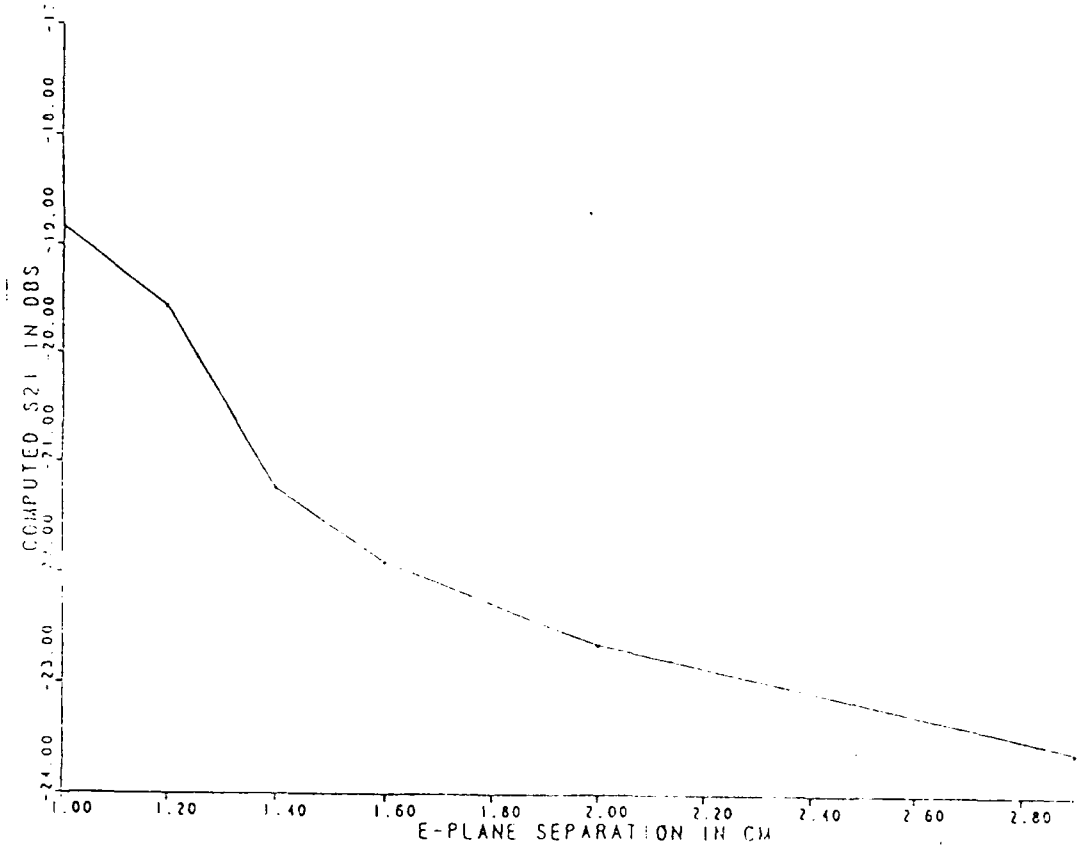

Figure 3.9: The S_{12} representation of the computed variation of the mutual impedance between two microstrip antennas (size 6 × 4 cm ; frequency = 2.35 GHz) as a function of distance in the E-plane

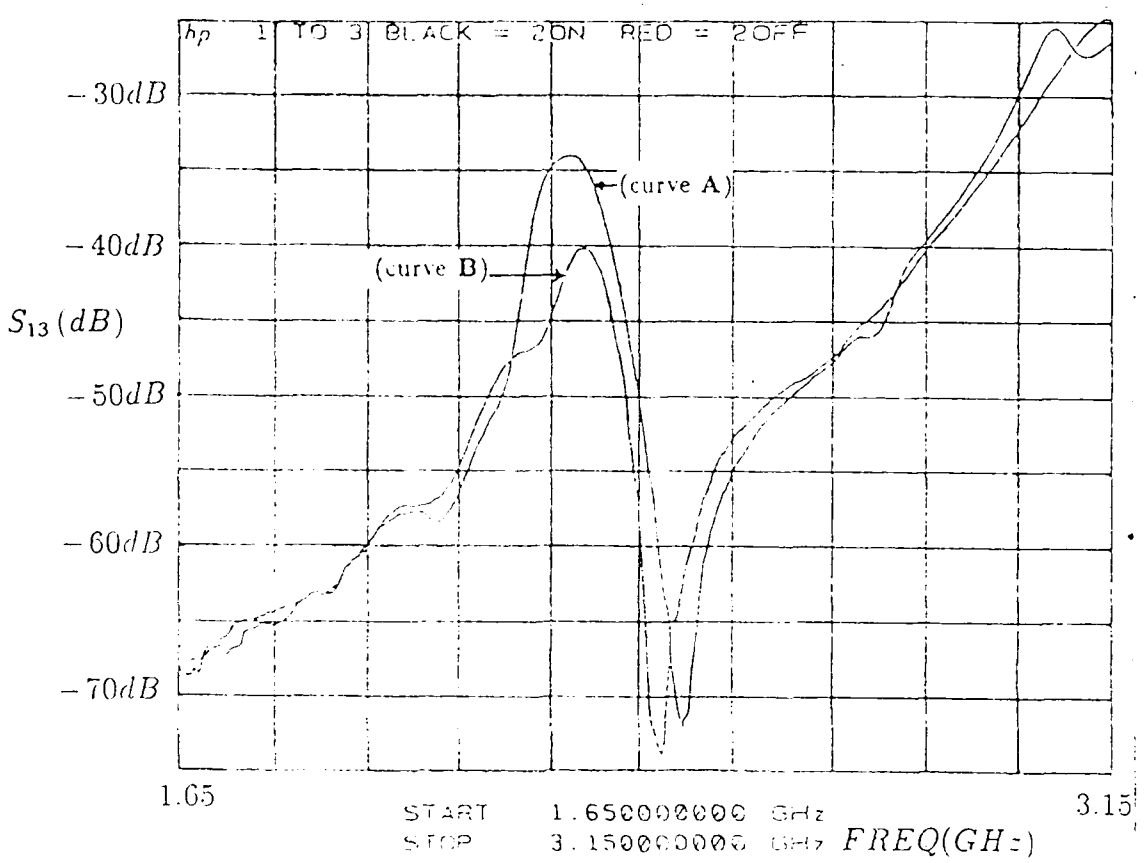

Figure 3.10: The measured S_{13} of a three patch linear array with the presence (curve A) and absence (curve B) of the second patch in the H-plane. Patch size 6 × 4 cm.; edge separation = 1cm ; feed position (1,1) ; resonant frequency = 2.35 GHz

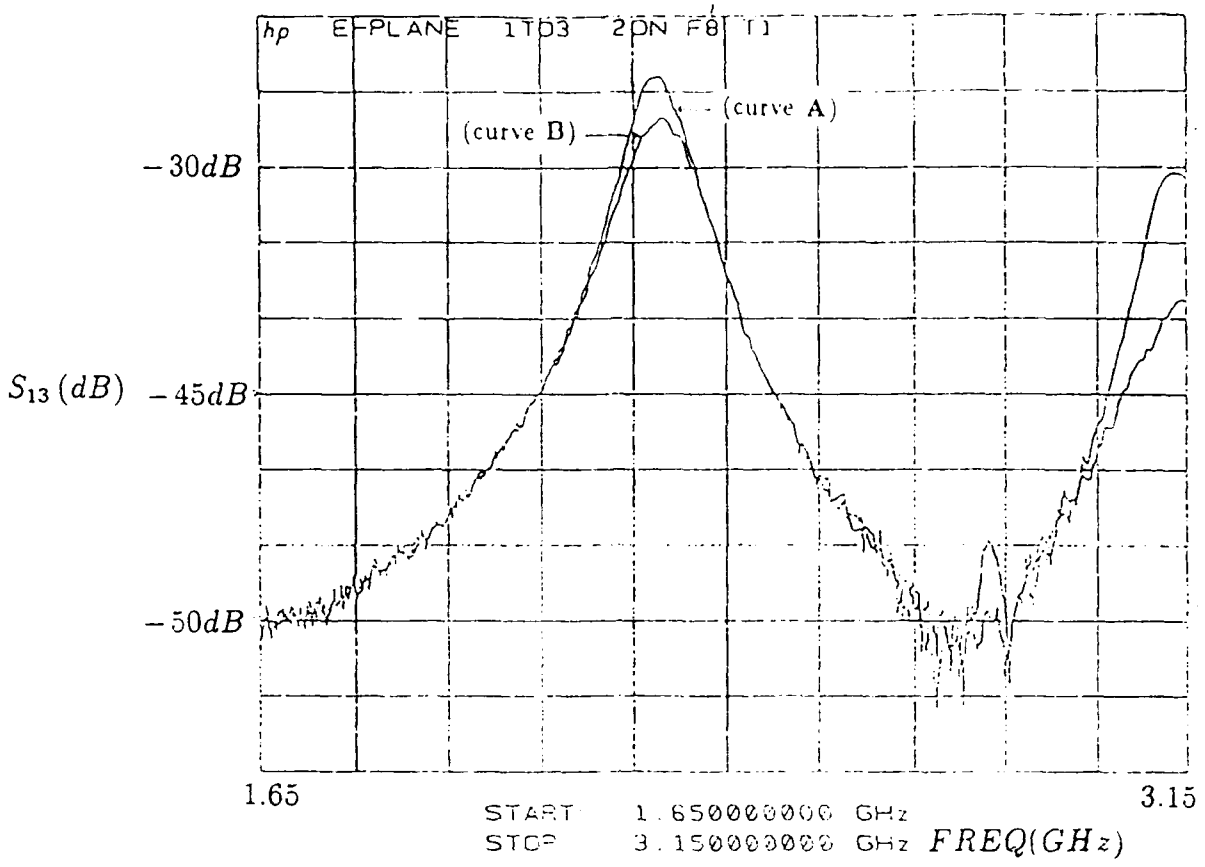

Figure 3.11: The measured S_{13} of a three patch linear array with the presence (curve A) and absence (curve B) of the second patch in the E-plane. Patch size 6 × 4 cm.; edge separation = 1cm ; feed position (1,1) ; resonant frequency = 2.35 GHz

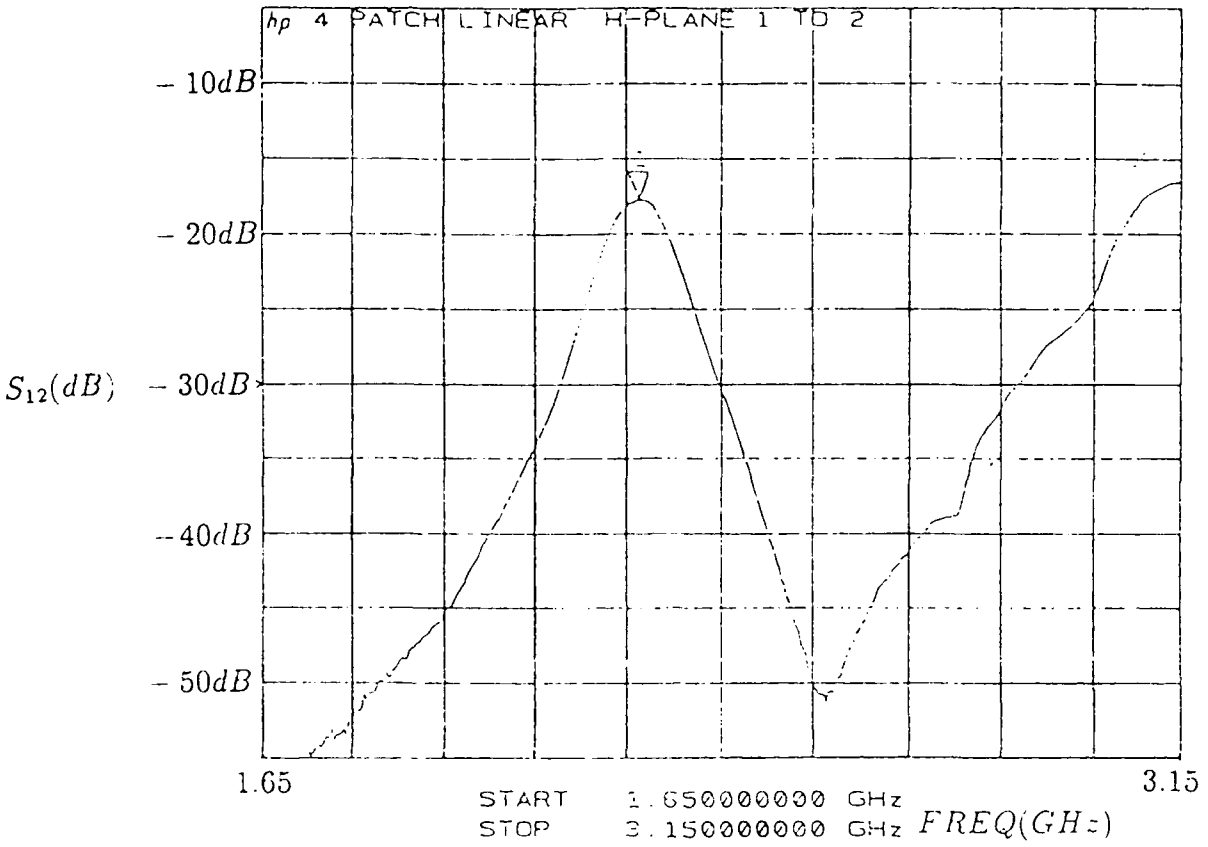

Figure 3.12. The measured S_{12} of a four patch linear array in the H-plane. Patch size 6 × 4 cm.; edge separation = 1cm ; feed position (1,1) ; resonant frequency = 2.35 GHz

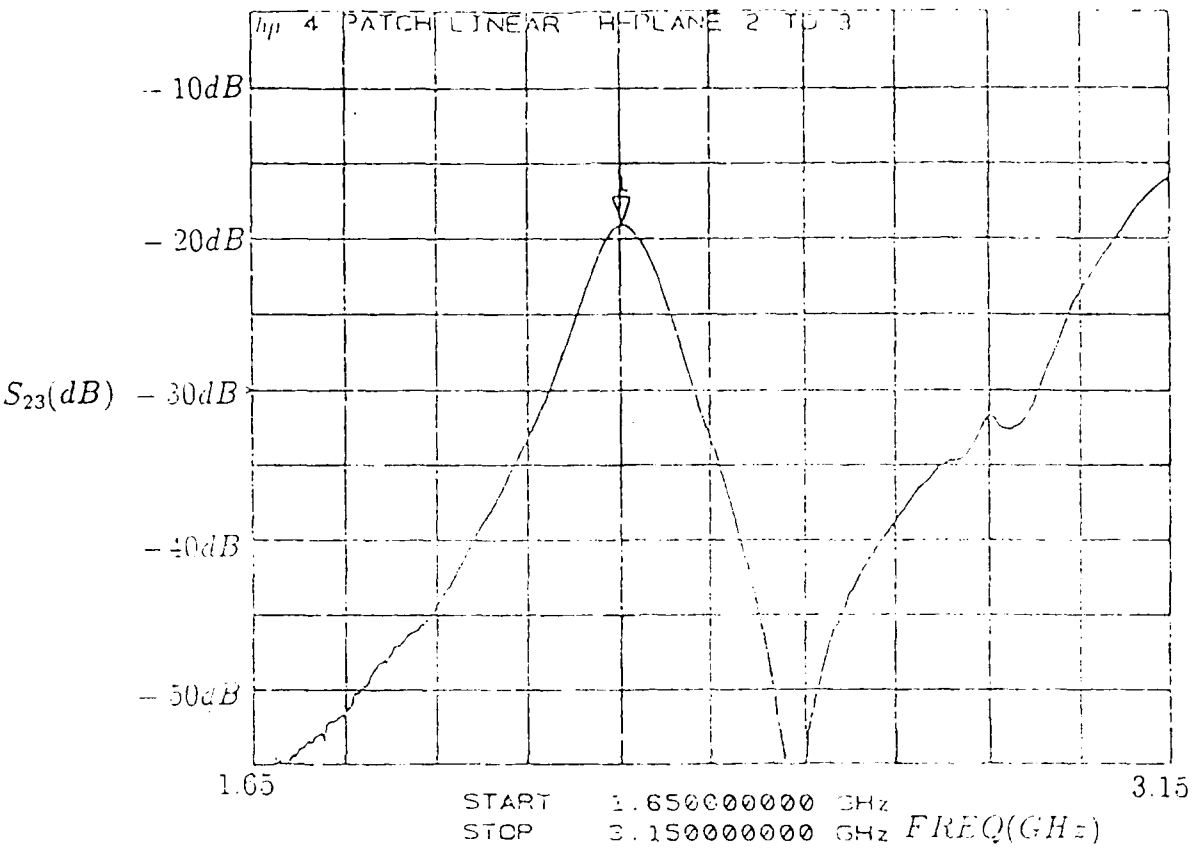

Figure 3.13: The measured S_{23} of a four patch linear array in the H-plane. Patch size 6 × 4 cm., edge separation = 1cm , feed position (1,1) ; resonant frequency = 2.35 GHz

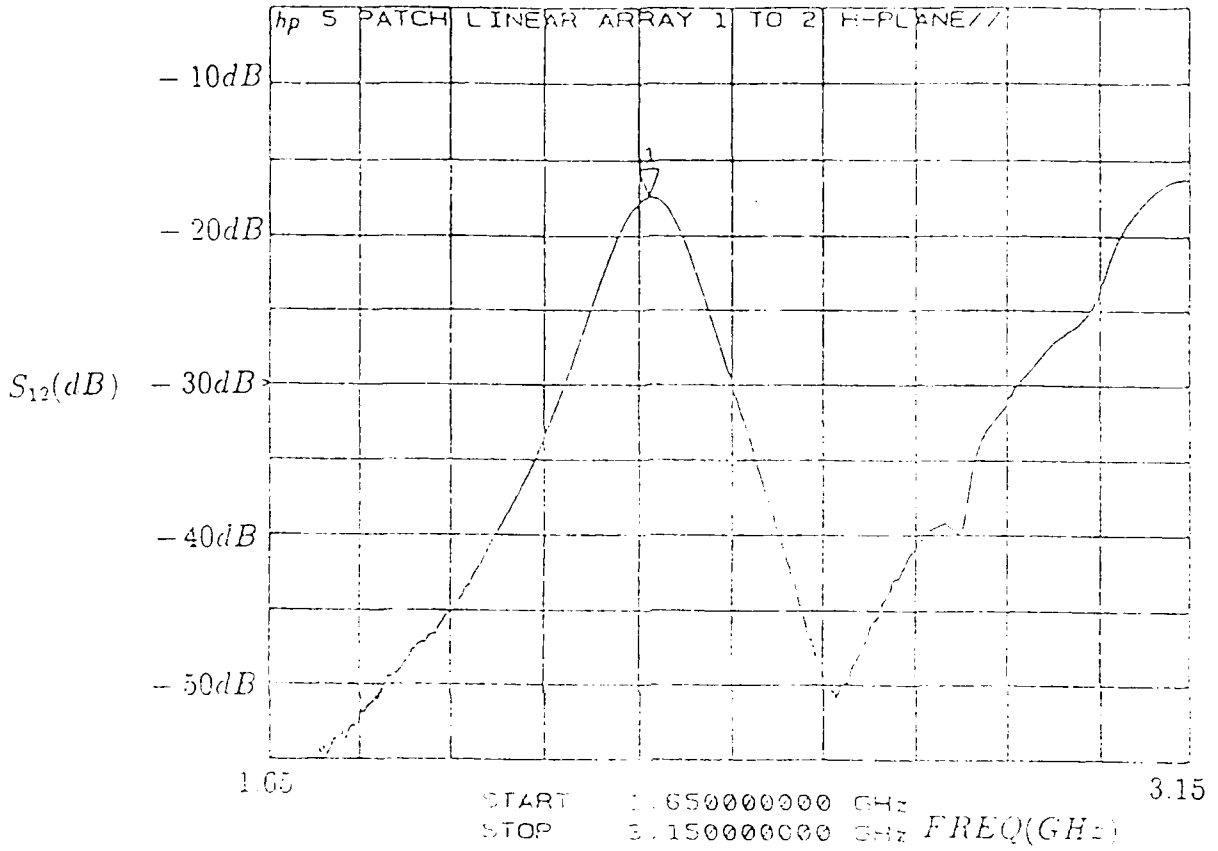

Figure 3.14: The measured S_{12} of a five patch linear array in the H-plane. Patch size 6 × 4 cm , edge separation = 1cm , feed position (1,1) ; resonant frequency = 2.35 GHz

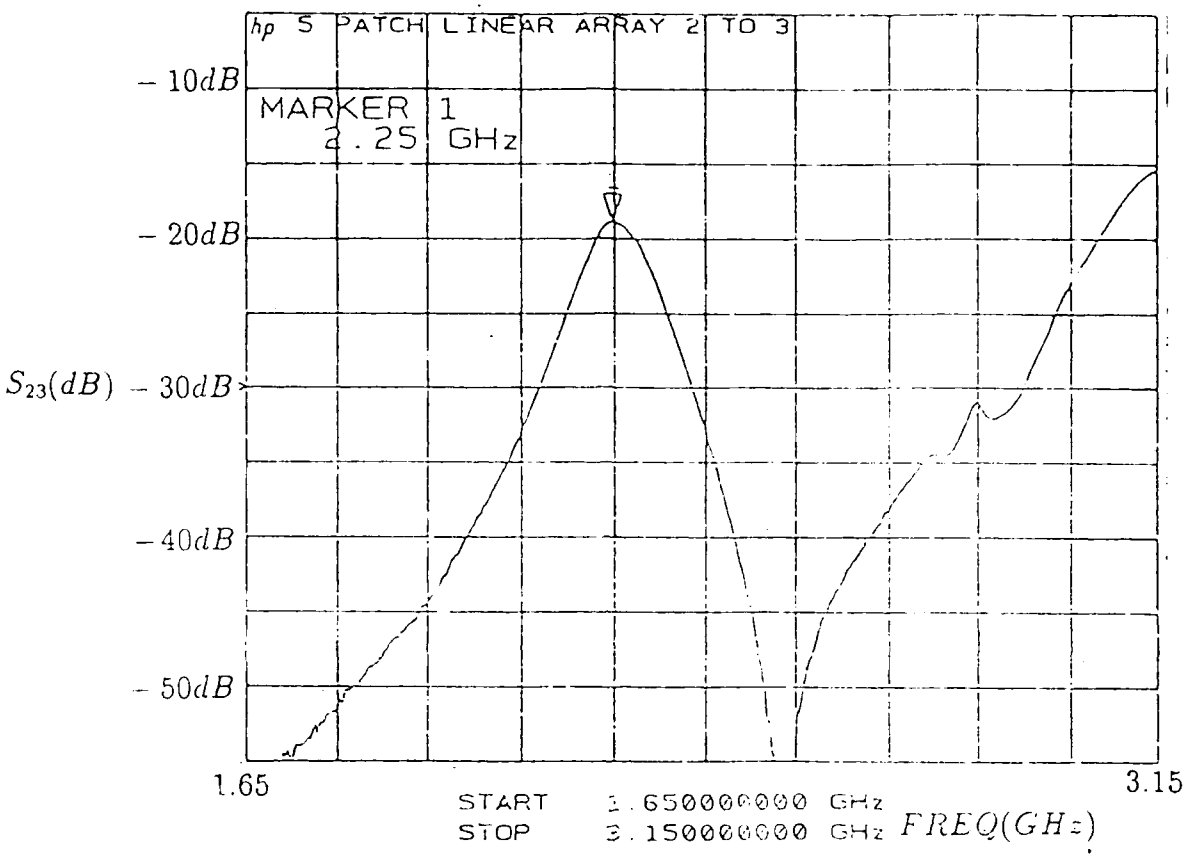

Figure 3.15: The measured S_{23} of a five patch linear array in the H-plane. Patch size 6 × 4 cm.; edge separation = 1cm , feed position (1,1) ; resonant frequency = 2.35 GHz

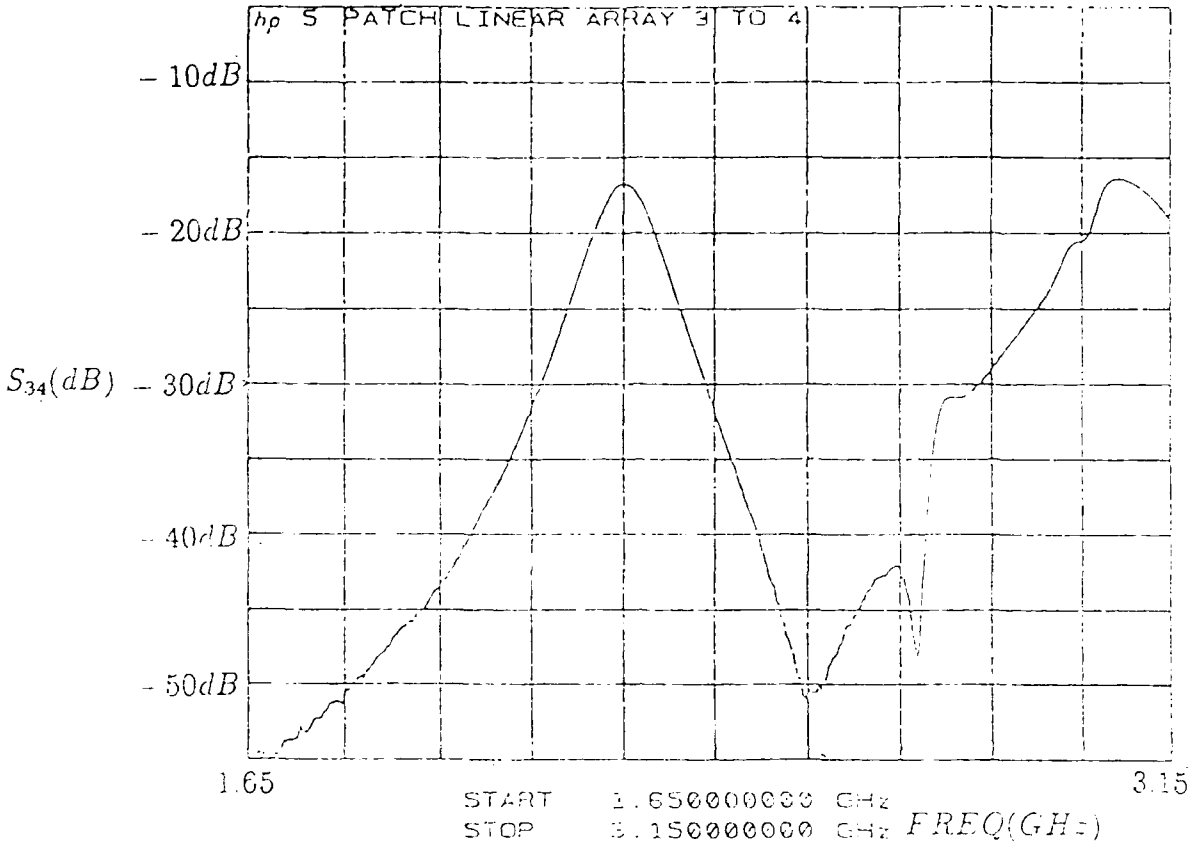

Figure 3.16: The measured S_{34} of a five patch linear array in the H-plane. Patch size 6 × 4 cm edge separation = 1cm ; feed position (1,1) ; resonant frequency = 2.35 GHz

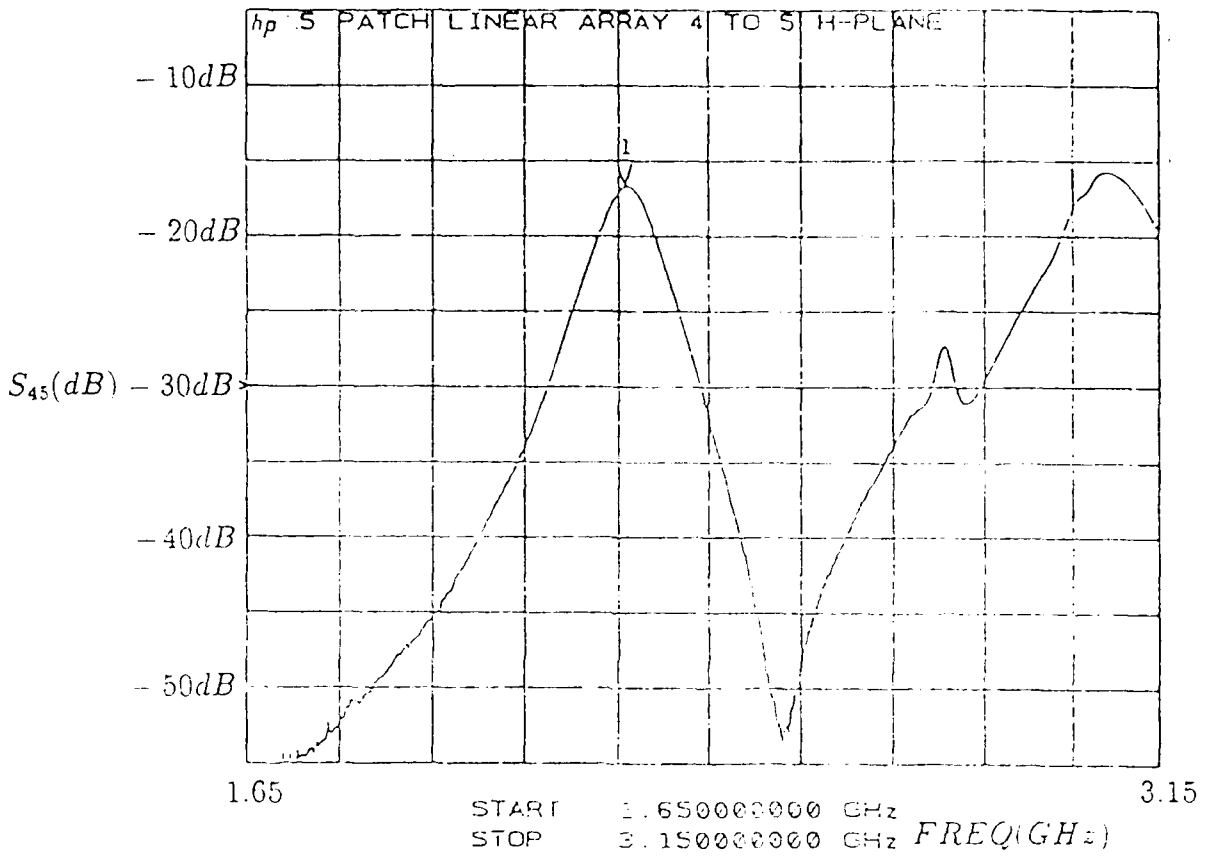

Figure 3.17: The measured S_{45} of a five patch linear array in the H-plane. Patch size 6 × 4 cm, edge separation = 1cm ; feed position (1,1) ; resonant frequency = 2.35 GHz

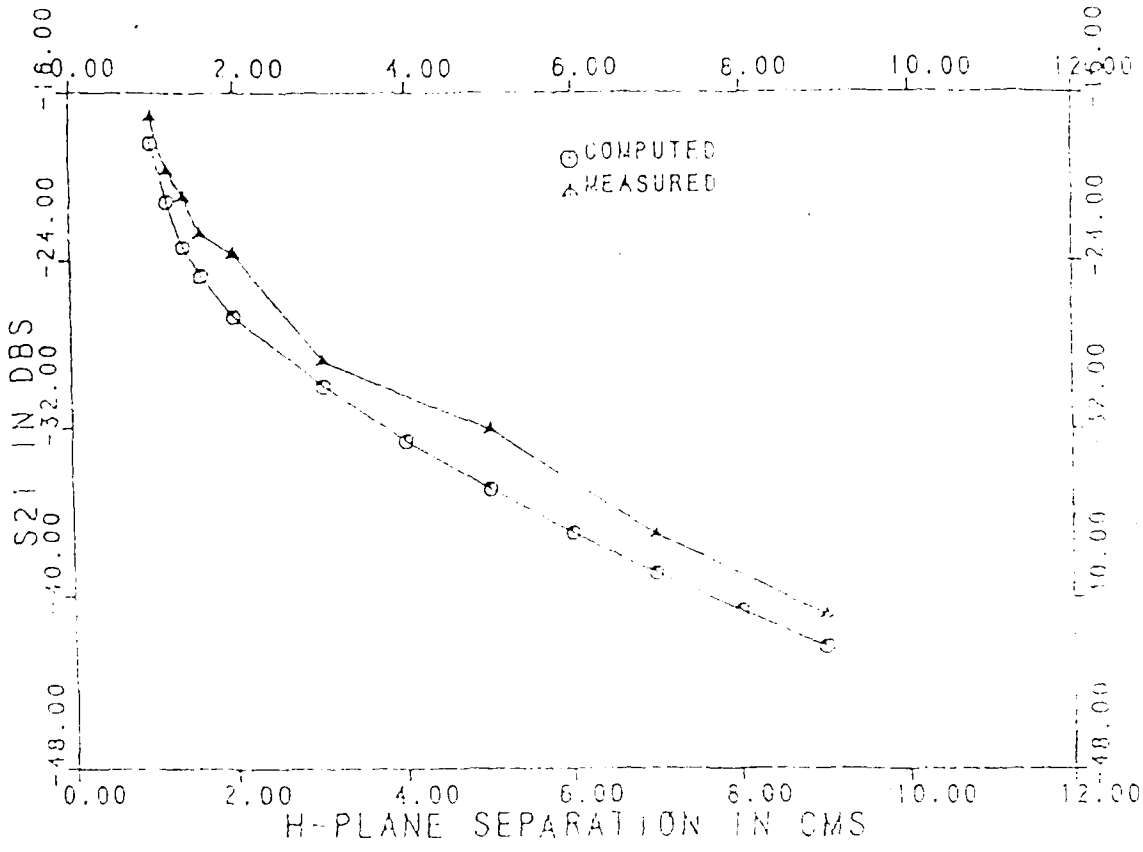

Figure 3.18: The computed and measured H-plane coupling in a two patch linear array. Patch size 6 × 4 cm.; edge separation = 1cm ; feed position (1,1) ; resonant frequency = 2.35 GHz

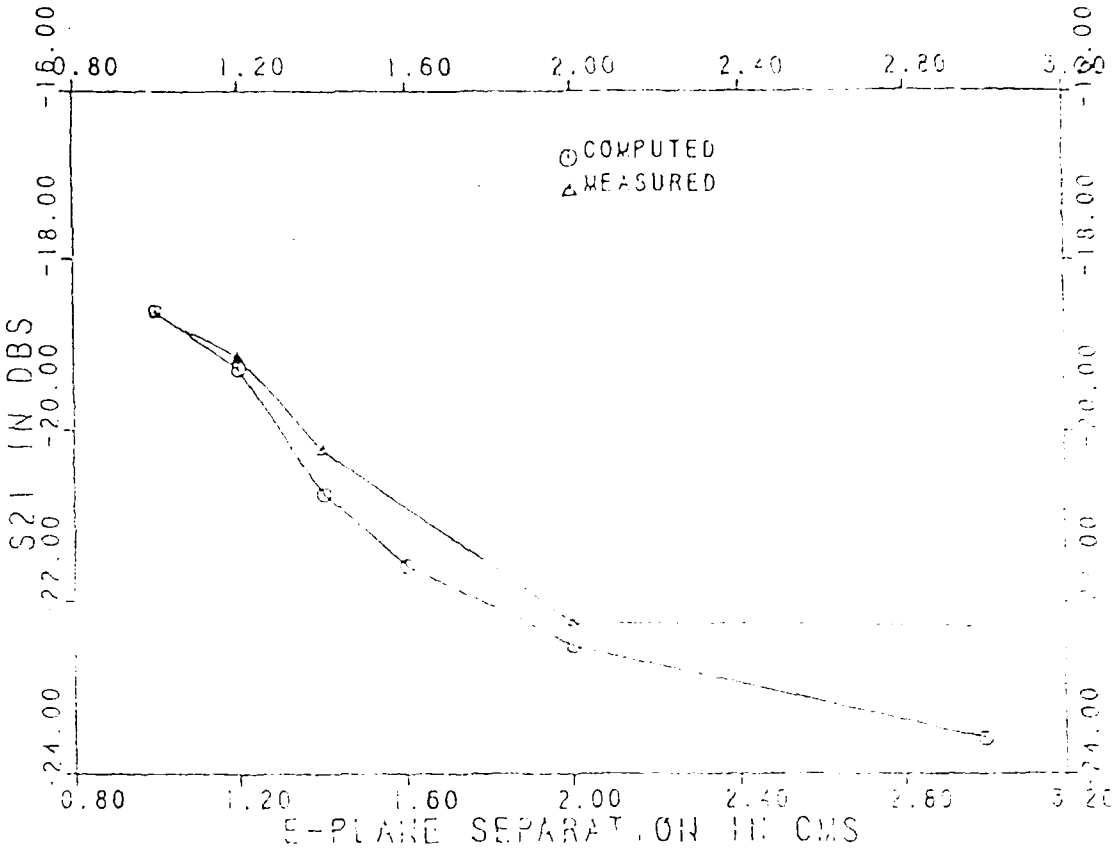

Figure 3.19. The computed and measured E-plane coupling in a two patch linear array. Patch size 6×4 cm.; edge separation = 1cm ; feed position (1,1) ; resonant frequency = 2.35 GHz

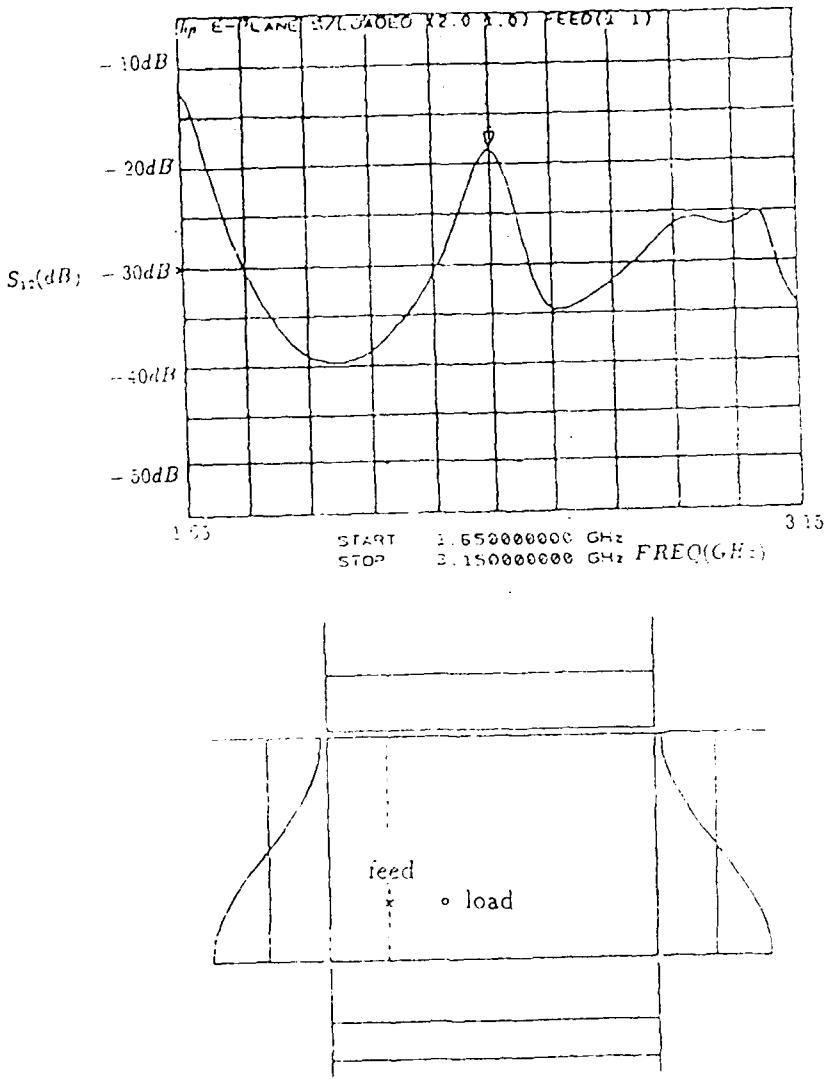

Figure 3.20: The measured E-plane coupling for a single loaded patch in a two patch linear array and its magnetic current distribution. Load positions : Patch1 (2.0,1.0) ; Patch2 (2.0,1.0) patch size 6 × 4 cm.; edge separation = 1cm ; feed position (1,1) ; resonant frequency = 2.35 GHz

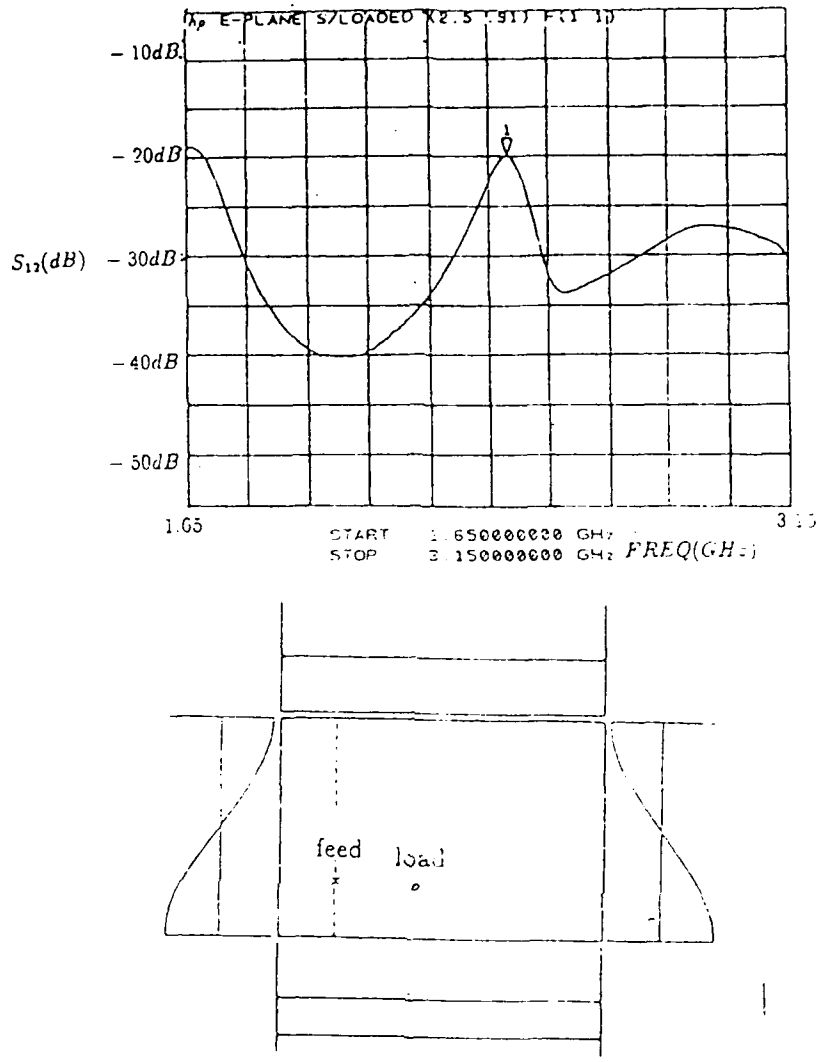

Figure 3.21: The measured E-plane coupling for a single loaded patch in a two patch linear array and its magnetic current distribution. Load positions: Patch1 (2.0,1.0) , Patch2 (2.5,0.91). patch size 6 × 4 cm.; edge separation = 1cm ; feed position (1,1) , resonant frequency = 2.35 GHz

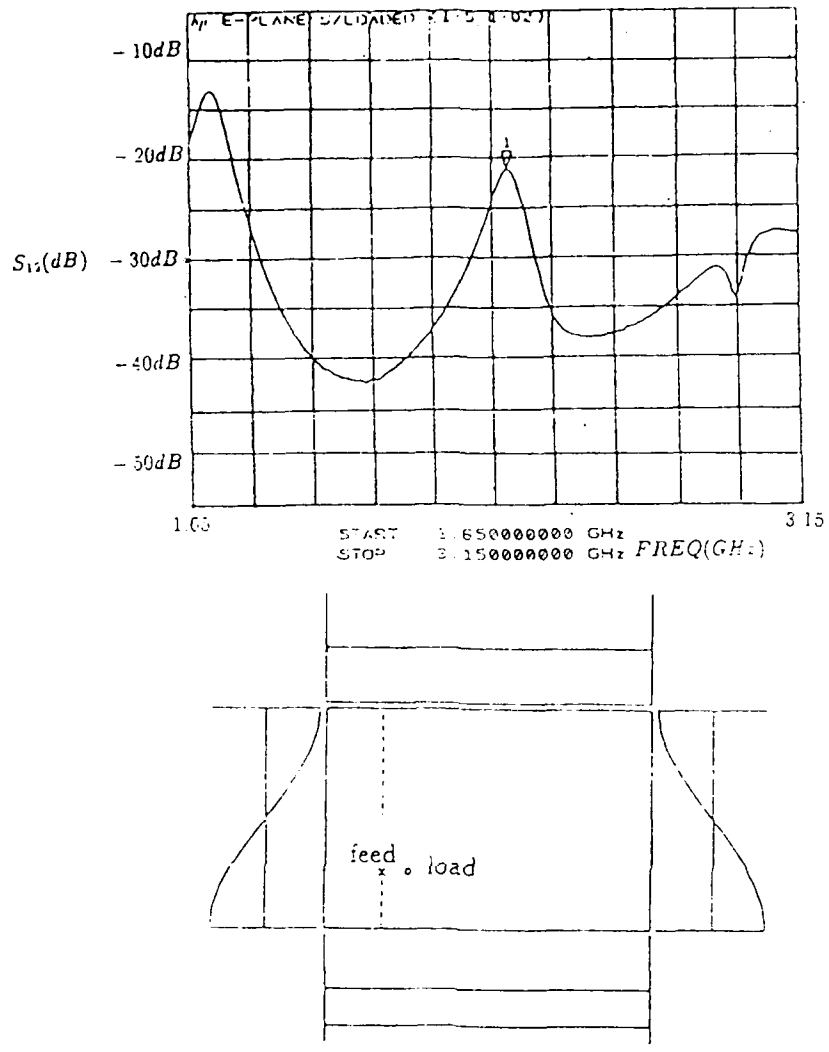

Figure 3.22: The measured E-plane coupling for a single loaded patch in a two patch linear array and its magnetic current distribution. Load positions: Patch1 (2.0,1.0) ; Patch2 (1.5,1.02). patch size 6 × 4 cm.; edge separation = 1cm ; feed position (1,1) ; resonant frequency = 2.35 GHz

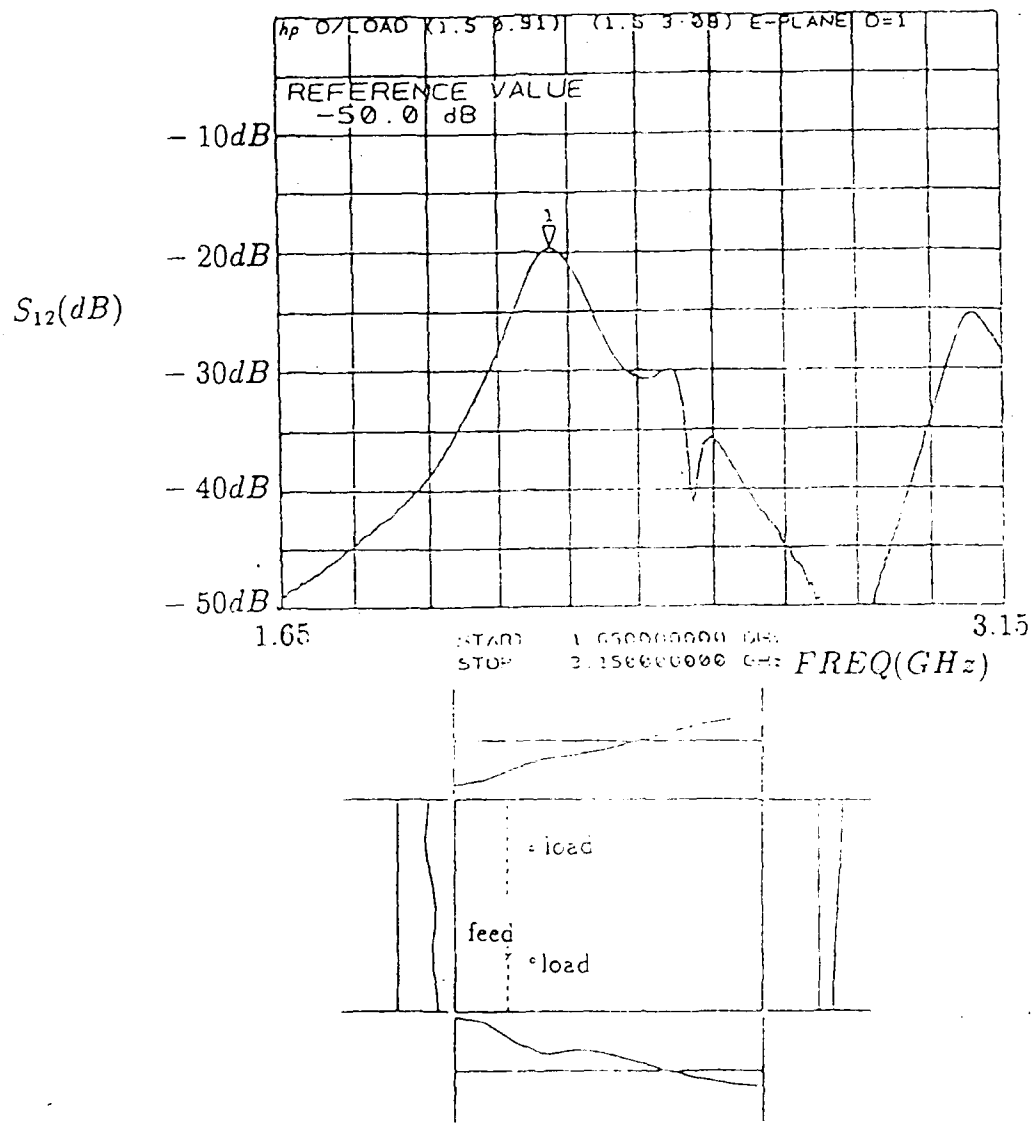

Figure 3.23: The measured E-plane coupling for a double loaded patch in a two patch linear array and its magnetic current distribution. Load positions: Patch1 (3.0,1.23) and (3.0,2.7) ; Patch2 (1.5,0.91) and (1.5,3.09) ; patch size 6 × 4 cm.; edge separation = 1cm ; feed position (1,1)

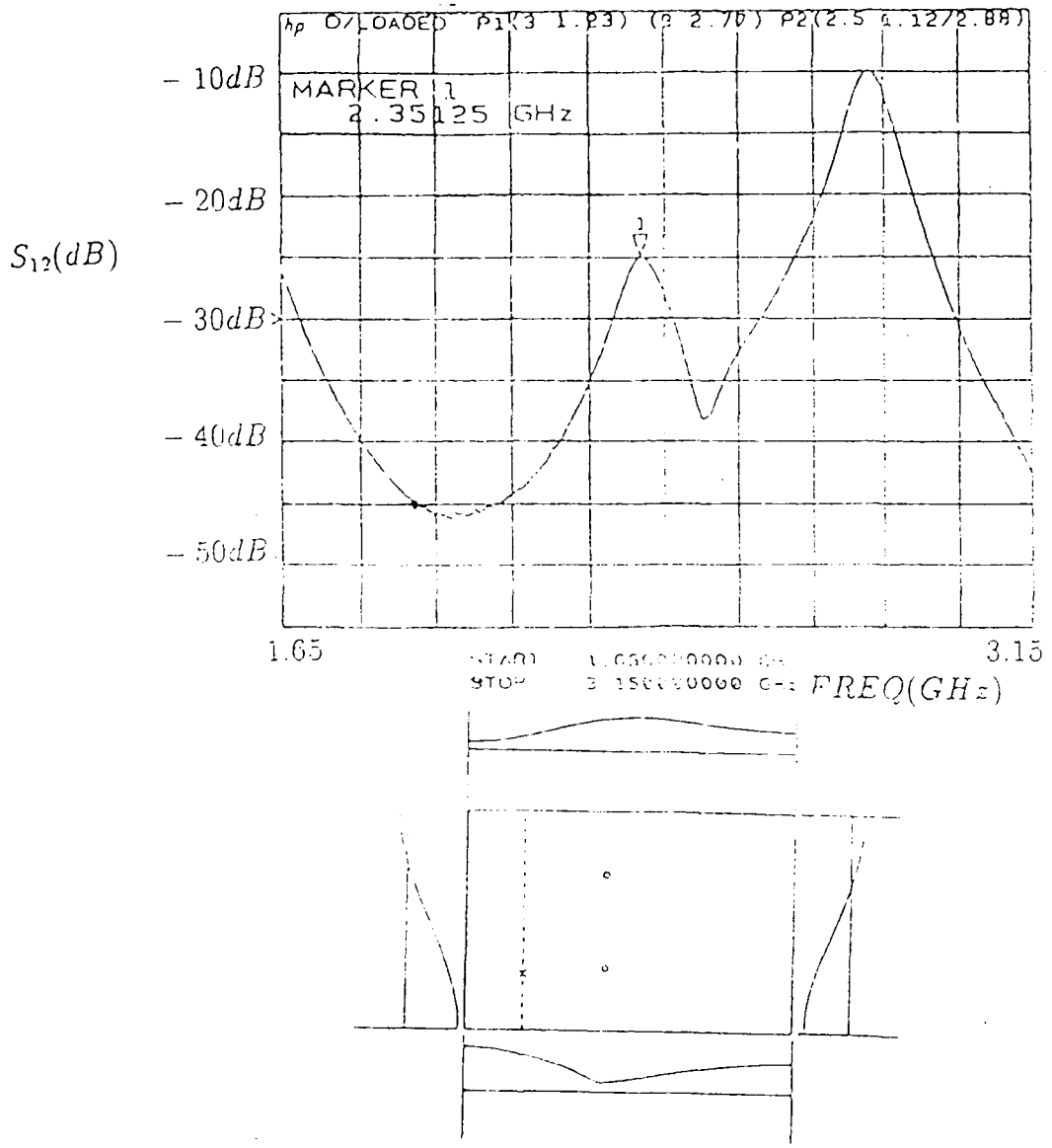

Figure 3.24: The measured E-plane coupling for a double loaded patch in a two patch linear array and its magnetic current distribution. Load positions: Patch1 (3.0,1.23) and (3.0,2.7). Patch2 (2.5,1.12) and (2.5,2.88); patch size 6 × 4 cm, edge separation = 1cm, feed position (1,1)

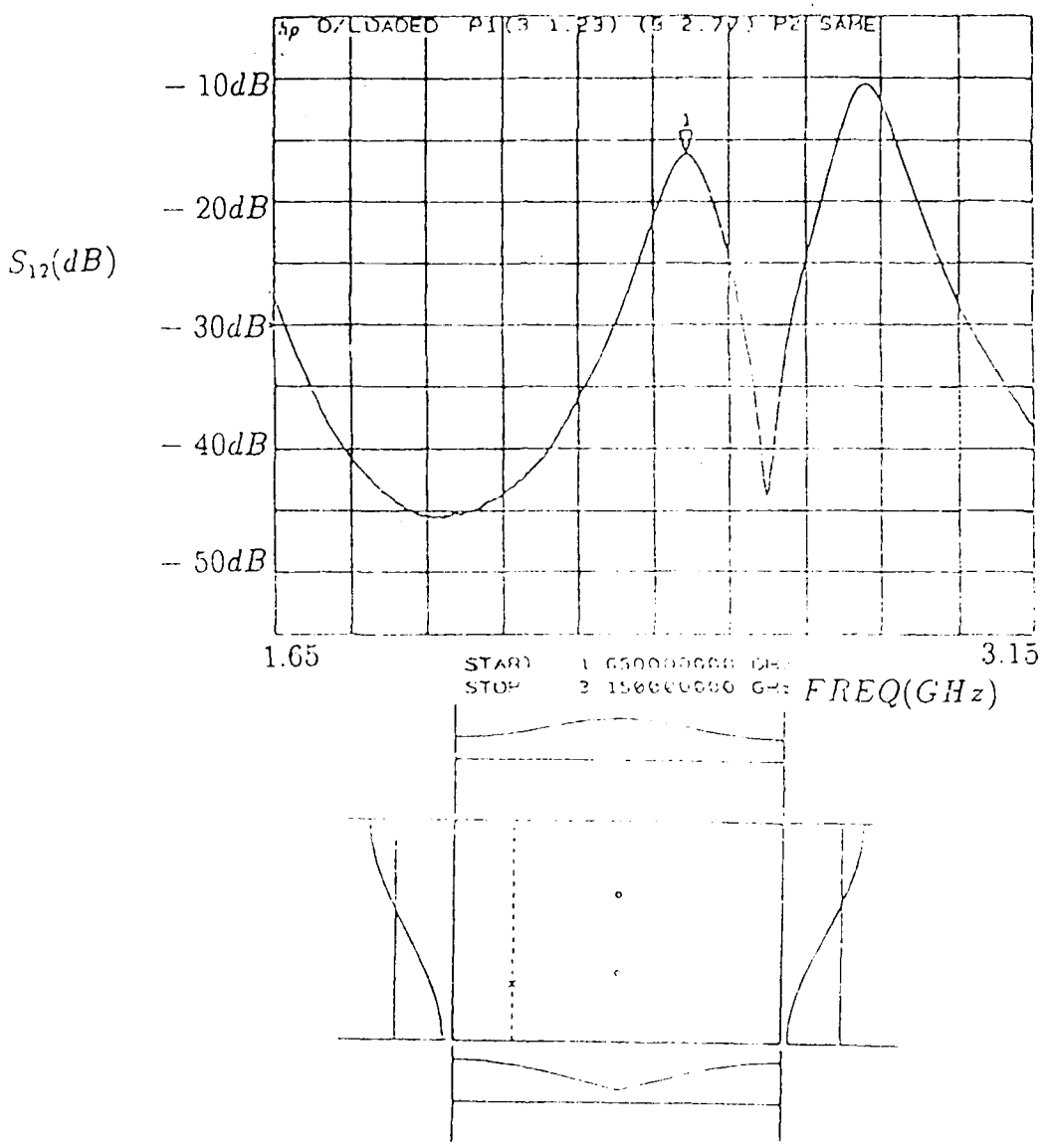

Figure 3.25: The measured E-plane coupling for a double loaded patch in a two patch linear array and its magnetic current distribution. Load positions: Patch1 (3.0,1.23) and (3.0,2.7) ; Patch2 (3.0,1.23) and (3.0,2.77) , patch size 6 × 4 cm., edge separation = 1cm , feed position (1,1)

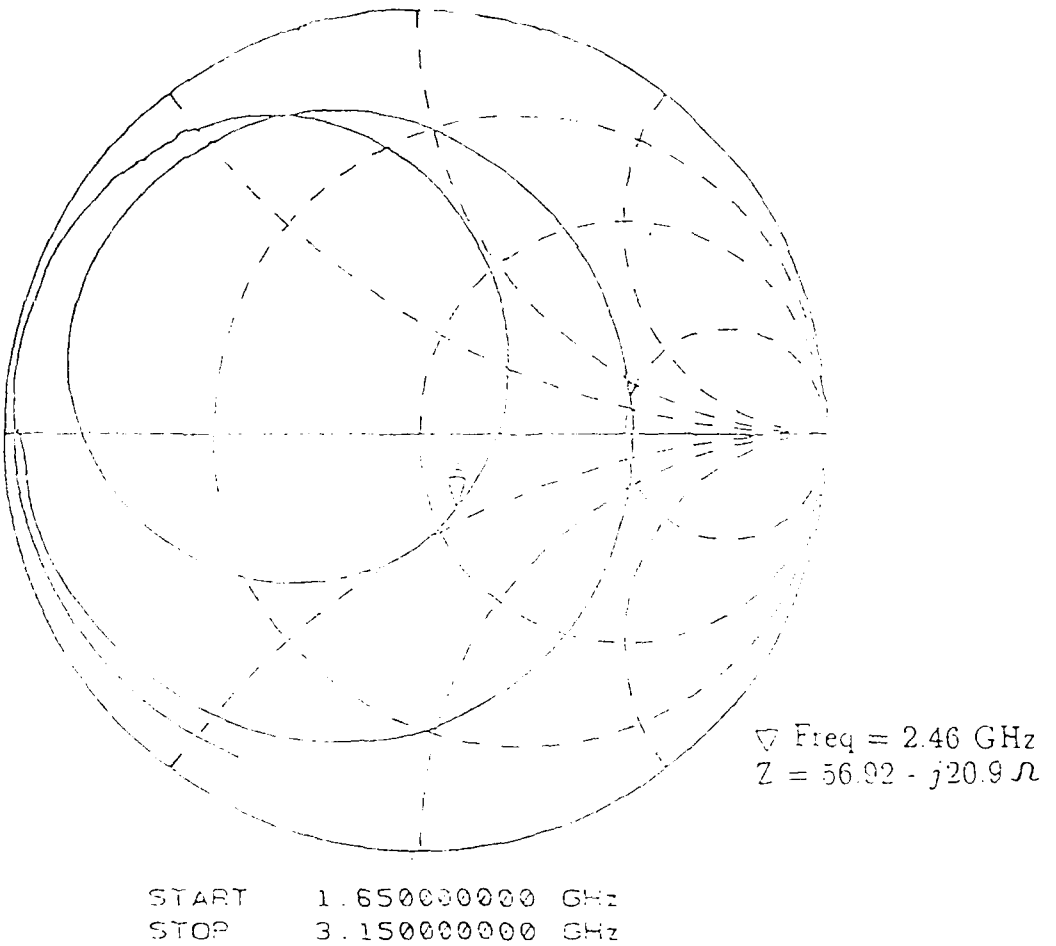

Figure 3.26: The measured S_{11} variation for a double loaded patch in a two patch linear array. Load positions: Patch1 (3.0,1.23) and (3.0,2.7) ; Patch2 (2.5,1.21) and (2.5,2.79) ; patch size 6 × 4 cm edge separation = 1cm , feed position (1,1)

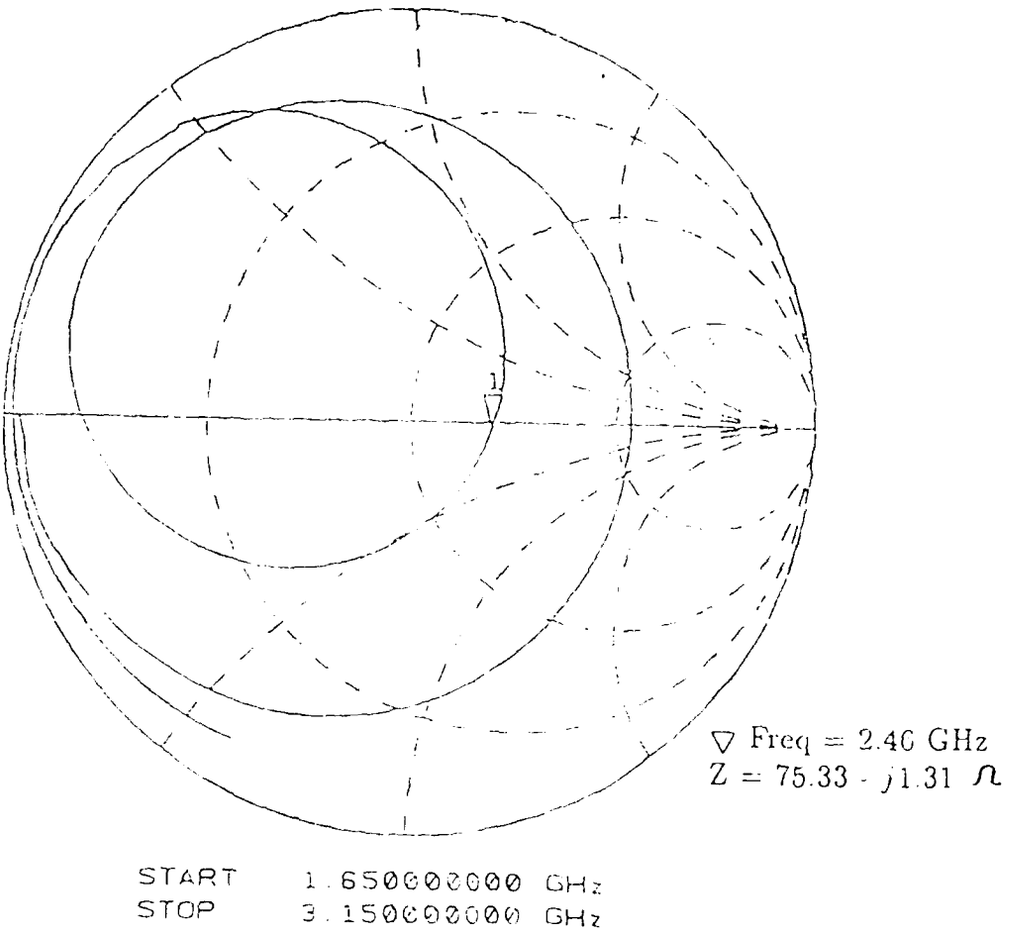

Figure 3.27: The measured S_{11} variation for a double loaded patch in a two patch linear array. Load positions: Patch1 (3.0,1.23) and (3.0,2.7) ; Patch2 (2.0,1.12) and (2.0,2.88) ; patch size 6 × 4 cm ; edge separation = 1cm ; feed position (1,1)

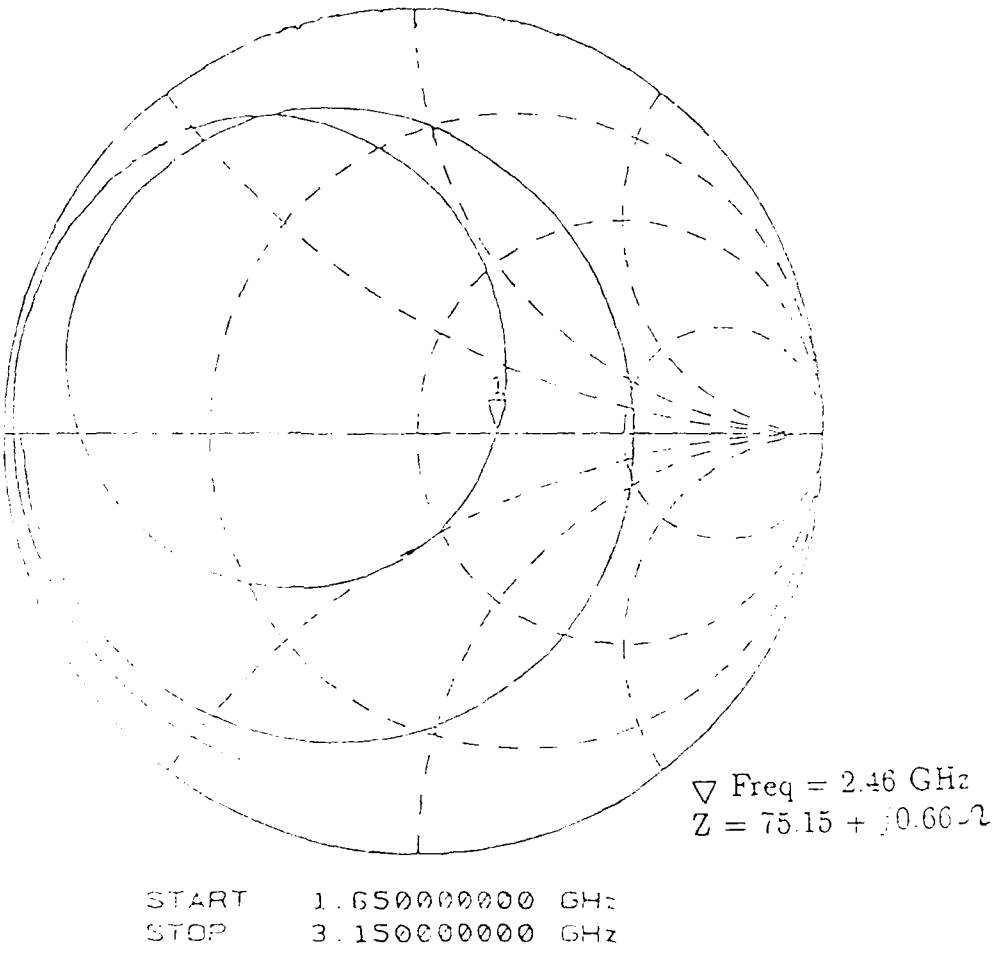

Figure 3.28: The measured S_{11} variation for a double loaded patch in a two patch linear array. Load positions: Patch1 (3.0,1.23) and (3.0,2.7) ; Patch2 (3.0,1.23) and (3.0,2.77) ; patch size 6 × 4 cm., edge separation = 1cm , feed position (1,1)

Chapter 4

USE OF REACTIVE LOADS FOR MAINTAINING IMPEDANCE MATCH IN SCANNED ARRAYS

It has been found that in an electronically scanned array of microstrip antennas the active driving point impedance of each element varies significantly when the array is scanned by either varying the progressive phase shift angle or by changing the frequency [11]. When this happens, the transmission feed lines that are usually matched to the array elements for maximum power transfer will experience a mismatch and consequently a large amount of power will be reflected back instead of radiating out. This reflected power is usually redirected by the circulator at the feed point and is coupled to an absorbing load to prevent it from going back to the transmitter. But this loss of power means loss of accuracy and range in a radar system.

The previous study of loaded microstrip antennas has revealed that the input impedance of an antenna can be changed by placing reactive loads at specific points

on the antenna so that the resonant frequency remains unaltered. It was the purpose of this study to see whether mutual coupling and the active impedance between microstrip antenna elements can be changed by positioning loads properly on the microstrip antenna. A program was written by the author to compute the mutual coupling using the loaded elements for a finite array. An approximate theory is used to compute mutual impedance between elements which did not consider the effect of other patch elements when computing the mutual coupling between any two elements. An exact expression should be used for accurate results as in [12] and [13]. For the purpose of the feasibility study the approximate model that was used was sufficient. The computed results were close to experimentally obtained values in most of the cases considered. The results, indicated that the mutual coupling and the input active impedance in an array can be varied by using loaded elements. This was verified experimentally and the results obtained are shown in Figures 3.23 to 3.28 of the previous chapter. A comparison of the computed and measured results is shown in Figure 4.1 for the E-plane linear array and Figure 4.2 for the H-plane linear array. A comparison of the computed and measured active impedance of two loaded patches in a linear array environment is shown in Figures 4.3 and 4.4.

The position of the reactive load on the antenna was computed to match the antenna elements at various scan angles as shown in Figure 4.5. The process is iterative because if one element is matched by changing its load position, then other elements of the array become mismatched. This requires changing the load position iteratively until a reasonable match is obtained for all the array elements.

A test case of a five-patch linear array was considered. It was initially assumed

that the array was matched when all port currents were in phase. As the progressive phase shift angle or the difference in phase angle between adjacent port currents is changed to 22.5°, 45° and 60°, the angle that the main beam makes with the broadside direction also changes. The load positions are changed to reduce mismatch. These load positions and the change in the magnitude of reflection coefficient are shown in Figure 4.5.

How much the performance of an array can be improved remains to be seen as this study continues, but from these results it does seem that an impedance match of array elements can be maintained within reasonable limits as beam scanning takes place.

MUTUAL COUPLING OF A TWO PATCH LINEAR ARRAY WITH LOADED PATCHES

E-Plane Dual Loads:

Load Positions:
Patch 1: Load1 (3.0 ,1.23) ; Load2 (3.0 ,2.7)
Patch 2: Load1 (1.5 ,0.91) : Load2 (1.5 ,3.09)
COMPUTED S21=-22.693 dBS ; MEASURED S21=-19.676 dBS

Load Positions:
Patch 1: Load1 (3.0 ,1.23) ; Load2 (3.0 ,2.77)
Patch 2: Load1 (2.5 ,1.12) : Load2 (2.5 ,2.88)
COMPUTED S21=-18.411 dBS ; MEASURED S21=-20.866 dBS

Load Positions:
Patch 1: Load1 (3.0 ,1.23) ; Load2 (3.0 ,2.77)
Patch 2: Load1 (3.0 ,1.23) : Load2 (2.0 ,2.77)
COMPUTED S21=-15.79 dBS ; MEASURED S21=-20.973 dBS

Figure 4.1: Table showing computed and measured values of the mutual coupling of two loaded patches in a linear array environment for the E-plane. Patch size 6 × 4 cm; edge separation = 1cm; feed position (1,1)

MUTUAL COUPLING OF A TWO PATCH LINEAR ARRAY WITH LOADED PATCHES
H-Plane Dual Loads:

Load Positions:
Patch 1: Load1 (3.0 ,1.23) ; Load2 (3.0 ,2.7)
Patch 2: Load1 (2.0 ,1.21) ; Load2 (2.0 ,2.79)
COMPUTED S21=-23.313 dBS ; MEASURED S21=-21.211 dBS

Load Positions:
Patch 1: Load1 (3.0 ,1.23) ; Load2 (3.0 ,2.77)
Patch 2: Load1 (2.5 ,1.12) ; Load2 (2.5 ,2.88)
COMPUTED S21=-24.447 dBS , MEASURED S21=-25.023 dBS

Load Positions
Patch 1: Load1 (3.0 ,1.23) ; Load2 (3.0 ,2.77)
Patch 2: Load1 (3.0 ,1.23) ; Load2 (2.0 ,2.77)
COMPUTED S21=-19.1364 dBS , MEASURED S21=-16.407 dBS

Figure 4.2 Table showing computed and measured values of the mutual coupling of two loaded patches in a linear array environment for the H-plane. Patch size 6 × 4 cm; edge separation = [illegible]; feed position (1,1)

ACTIVE IMPEDANCE OF A TWO PATCH LINEAR ARRAY WITH LOADED PATCHES
H-Plane Dual Loads

Load Positions
Patch 1: Load1 (3.0 ,1.23) ; Load2 (3.0 ,2.7)
Patch 2: Load1 (2.0 ,1.21) ; Load2 (2.0 ,2.79)
MEASURED Z_{active} = 75.336 - j1.312

Load Positions
Patch 1: Load1 (3.0 ,1.23) ; Load2 (3.0 ,2.77)
Patch 2: Load1 (2.5 ,1.12) ; Load2 (2.5 ,2.88)
MEASURED Z_{active} = 56.996 - j20.910

Load Positions
Patch 1: Load1 (3.0 ,1.23) ; Load2 (3.0 ,2.77)
Patch 2: Load1 (3.0 ,1.23) ; Load2 (2.0 ,2.77)
MEASURED Z_{active} = 75.152 + j0.66

Figure 4.3: Table showing measured values of active impedance of two loaded patches in a linear array environment for the H-plane. Patch size 6 × 4 cm; edge separation = 1cm; feed position (1,1)

ACTIVE IMPEDANCE OF A TWO PATCH LINEAR ARRAY WITH LOADED PATCHES

E-Plane single Loads.

Load Positions:
Patch 1: Load1 (2.0 , 1.0)
Patch 2: Load1 (1.5 , 1.02)
MEASURED Z_{active} = 78.934 + j0.449

Load Positions:
Patch 1: Load1 (2.0 , 1.0)
Patch 2: Load1 (2.0 , 1.0)
MEASURED Z_{active} = 40.461 + j0.5527

Load Positions:
Patch 1: Load1 (2.0 , 1.0)
Patch 2: Load1 (2.5 , 0.91)
MEASURED Z_{active} = 51.66 + j0.5527

Figure 4.4: Table showing measured values of active impedance of two loaded patches in a linear array environment for the E-plane. Patch size 6 × 4 cm; edge separation = 1cm; feed position (1,1)

progressive phase shift	0.0	22.5	45.0
	* 0.00	* 0.179	* 0.30
	* 0.00	* 0.102	* 0.228
	* 0.00	* 5.17E-2	* 0.185
	* 0.00	* 4.48E-2	* 0.147
	* 0.00	* 0.12	* 0.122

input reflection coefficient before matching

progressive phase shift	0.0	22.5	45.0
1	* 0.00	** 0.147	*** 9.79E-2
2	* 0.00	** 5.09E-2	*** 9.2E-2
3	* 0.00	** 4.37E-2	** 1.45E-2
4	* 0.00	** 5.66E-2	** 2.1E-2
5	* 0.00	** 2.25E-2	*** 1.75E-2

input reflection coefficient after matching

LOAD POSITIONS

* (1.5,1.17) ; (1.5,2.83)

** (2.25,1.12) , (2.25,2.88)

*** (2.75,1.17) , (2.75,2.83)

Figure 4.5: Table showing the computed position of short circuit loads required to keep the microstrip antenna patches in a 5 patch element linear phased array matched to the feed network. The array is assumed to be matched at a progressive phase shift angle of 0°. Patch size 5 × 4 cm ; edge separation = 1cm ; feed position (1,1)

Chapter 5

CONCLUSIONS

The experimental study of loaded microstrip antennas showed that the properties of microstrip antennas can be changed quite easily to suit a given set of applications. By placing reactive loads on the microstrip antenna one can change its resonant frequency and input impedance. If these loads are placed appropriately, then it is possible to change only the input impedance of the antenna without changing the resonant frequency.

The theoretical and experimental study of microstrip antenna arrays showed that the active impedance of an array element is affected significantly by the mutual coupling effects of surrounding elements. This active impedance was found to vary with scan angle in phase scanned arrays. This causes an impedance mismatch at the feed point of array elements resulting in a loss of radiated power due to reflections. The feasibility study on the use of loaded microstrip antennas to reduce the mismatch of these elements in a scanned array showed that dynamic controlling of input impedance of array elements is possible. This can be achieved by appropriately changing the reactive load position as phase scanning takes place.

The reactive loads could be short circuits for which PIN diodes can be used allowing switching appropriately from a computer during phase scanning.

Bibliography

[1] I. J. Bahl, P. Bhartia, "Microstrip Antennas ", Artech House, Inc. 1982, pp. 4-80.

[2] W. F. Richards, Shayla E. Davidson, S.A. Long, 'Dual band reactively loaded microstrip antennas", *IEEE Trans. on Antennas and Prop.*, Vol. AP-33, No. 5, May 1985, p. 556.

[3] W. F Richards, Y.T. Lo, D.D. Harrison, "An improved theory for microstrip antennas and applications", *IEEE Trans. on Antennas and Prop.* , Vol. AP-29, No. 1, January 1981, pp. 38-46.

[4] W. F. Richards, Stuart A. Long, "Adaptive pattern control of a reactively loaded, dual mode microstrip antenna", *International Telemetry Conference Proceedings*, Las Vegas, Nevada, October 1986, pp. 291-296.

[5] W. F. Richards, Stuart A. Long, "Impedance control of microstrip antennas utilizing reactive loading", *International Telemetry Conference Proceedings*, Las Vegas, Nevada, October 1986, pp. 285-296.

[6] K. G. Schroeder, "Miniature slotted-cylinder antennas", *Microwaves*, Vol.3, December 1964, pp. 28-37.

[7] W. F. Richards, "Dynamic control of the input impedance of a microstrip antenna using loaded elements", Technical Report 86-11, Applied Electromagnetics Laboratory, Department of Electrical Engineering, University of Houston, 1986.

[8] Robert E. Collin, Francis J. Zucker, editors, "Antenna theory", part 1 and 2, McGraw Hill, 1969.

[9] Sheng-fuh R. Chang, "Mutual coupling between microstrip antennas with arbitrary spacing and orientation", *IEEE Trans. on Antennas and Prop.* (to be published)

[10] D. R. Jackson, W. F. Richards and Ajaz Ali-Khan, "An exact coupling theory for microstrip patches", *IEEE Trans. on Antennas and Prop.*, (to be published)

[11] R. C. Hansen, "Significant phased array papers", Artech House, 1973.

[12] David M. Pozar, "Finite phased arrays of microstrip patches", *IEEE Trans. on Antennas and Prop.*, Vol. AP-34, No. 5, May 1986, pp. 658-665.

[13] R. P. Jedlicka, K. R. Carver, "Mutual coupling between microstrip antennas" Proceedings on the workshop on printed circuit antenna technology, New Mexico State University, Las Cruces, New Mexico 1979, pp. 4.1-4.8.

MISSION
of
Rome Air Development Center

RADC plans and executes research, development, test and selected acquisition programs in support of Command, Control, Communications and Intelligence (C^3I) activities. Technical and engineering support within areas of competence is provided to ESD Program Offices (POs) and other ESD elements to perform effective acquisition of C^3I systems. The areas of technical competence include communications, command and control, battle management information processing, surveillance sensors, intelligence data collection and handling, solid state sciences, electromagnetics, and propagation, and electronic reliability/maintainability and compatibility.